Development of a Single-Stage Modulator for Comprehensive Two-Dimensional Gas Chromatography (GC × GC)

by

Christopher McNeish

A thesis
presented to the University of Waterloo
in fulfillment of the
thesis requirement for the degree of
Master of Science
in
Chemistry

Waterloo, Ontario, Canada, 2011

AUTHOR'S DECLARATION

I hereby declare that I am the sole author of this thesis. This is a true copy of the thesis, including any required final revisions, as accepted by my examiners.

I understand that my thesis may be made electronically available to the public.

Abstract

The ability to effectively analyze particulate matter ($PM_{2.5}$) in air is becoming increasingly pertinent. Allen Goldstein of the University of California in Berkeley is studying the semi-volatile fraction of organic compounds in $PM_{2.5}$ through the use of the thermal desorption aerosol gas chromatograph (TAG) system. However, as conventional GC does not provide adequate separation power, the development of comprehensive two-dimensional gas chromatography (GC × GC) was required. GC × GC works more effectively by utilizing a modulator that periodically traps and focuses analytes from a primary column onto a secondary column. This allows for the primary and secondary columns to separate the analytes based on two different properties.

This report focuses on the continuing study and enhancement of a modulator designed by Ognjen Panić during his Masters project. Improving and testing the robustness of this dual stage modulator was originally the focus of this project. However, this study led to the development of a single stage modulator. In addition to that, the effect of modulator characteristics such as length of the restriction, total length of the modulator and wall thickness on the modulator performance were studied. A robustness test of the single stage modulator was also completed. Experiments conducted tested the characteristics of the new modulator to ensure it performed effectively and would satisfy the requirements of the TAG system. A study comparing the sensitivity of conventional gas chromatography and GC × GC was also preformed. The sensitivity of GC × GC was on average an order of magnitude better than that of 1D GC.

Acknowledgements

I would first like to thank my supervisor Dr. Tadeusz Górecki. His willingness to provide advice on both an academic and a personal level was much of the reason I was able to complete this project. To him, I would like to express my sincerest gratitude.

Secondly, I would like to thank my fellow collaborators, Dr. Allen Goldstein and his associates from the University of California at Berkeley. Their support and advice was always appreciated.

This project would not have been possible without the numerous hours of guidance and support from the University of Waterloo's Science and Technical Services (STS). A special thanks to Jaeck Szubra and Harmen Vander Heide for enriching me with their years of experience.

Also, I am thankful to all of the past and present group members that have helped me along my journey. There was always someone around to bounce an idea off of or just to have a laugh. I am especially grateful to Ognjen Panic for all of his support during the inception of this project. In addition, I would like to extend a very special thank you to Dr. Suresh Seethapathy for his countless hours of professional consultation and personal advice.

In addition, I would like to thank my rather large family for their years of support and encouragement, even when they did not understand a word I was saying.

Finally, I would like to dedicate this thesis to my future wife Amanda Ma, who makes me feel like there is nothing I can not do.

Table of Contents

List of Figures

List of Tables

.

Chapter 1
Introduction

A growing concern for air quality, especially in urban areas, is currently evident. This concern has sparked much research in the scientific realm. The Takegawa group at the University of Tokyo, Japan, for example, are studying atmospheric aerosols with their Aerodyne Aerosol Mass Spectrometer (AMS).[1] Furthermore, the Zimmermann group from the University of Augsburg, Germany are utilizing gas chromatography-mass spectrometry (GC-MS), and more recently, comprehensive two-dimensional gas chromatography-mass spectrometry (GC × GC-MS) to analyze the semi-volatile fraction of the organic particulate matter in the air.[2] Particulate matter (PM), being a mixture of many compounds that are in their solid or liquid phases, can come in a variety of shapes, sizes, surface areas, solubilities, and origins.[3] Organic particulate matter is a key component in studying air quality as trace components from such environmental contaminants as motor vehicles, wood combustion, meat charbroiling, tire dust, and cigarette smoke can be found in them.[4] Organic particulate matter with diameter smaller than 2.5 μm, or $PM_{2.5}$, typically makes up about 20 – 80% of the mass of atmospheric aerosols and is of specific concern.[5] This concern stems from the negative effects of $PM_{2.5}$ on human health, which include hospitalizations due to lung function and respiratory symptoms, and even mortality.[3]

The composition of aerosols is not constant throughout the day: as the day goes on, different factors change the makeup of the aerosols. For example, variable traffic patterns occur during different times of the day, and changes in factory emissions result from varying intensities of use during manufacturing processes. Sampling of airborne particulate matter is carried out using both active and passive methods; in the latter case, the process can take several weeks,[6,7]

depending on the analyte. This is not ideal for determining variable changes in the composition of aerosols, or of the timing of emissions. Emissions may also contain compounds characteristic of the source, which may be beneficial in providing information with regards to the origin and timing of the emission.

The chemical characterization of $PM_{2.5}$ is a very important topic due to the reasons explained above. One of the groups actively involved in this area of study is that of Prof. Allen Goldstein of the University of California in Berkeley.[5] His group has developed a field instrument to characterize semi-volatile organic compounds in $PM_{2.5}$ in a semi-continuous manner, in order to determine the changes in their composition over time. The instrument, called the thermal desorption aerosol gas chromatograph-mass spectrometer (TAG), works by using an impactor to collect particles. The semi-volatile organic fraction is then thermally desorbed and analyzed with a gas chromatograph-mass spectrometer (GC-MS). The air is first filtered and then the particles are collected in a collection-desorption cell (CTD). Afterwards, the particles are thermally desorbed, and the semi-volatile organic fraction is carried into the GC-MS with helium carrier gas. This method has been successful in identifying many compounds in particulate matter such as alkanoic acids, alkanes (C_{17} to C_{35}), and polycyclic aromatic hydrocarbons (PAHs). [8] However, as with many complex mixtures, many of the analytes co-elute, which makes it difficult or even impossible to determine each compound's identity.

The best solution to the common problem of co-elution in one-dimensional gas chromatography (1D-GC) is comprehensive two-dimensional gas chromatography (GC × GC). GC × GC provides additional peak capacity, as well as separates components based on two different properties, such as volatility and polarity. By replacing 1D-GC with GC × GC in the

TAG system (2D-TAG), additional compounds can be characterized. These newly characterized compounds can thus be used to provide a better understanding of the source and timing of the emissions.

The TAG system is primarily used for field campaigns. As such, it is important for the 2D-TAG system to also function effectively in the field. To ensure the 2D-TAG system is field capable, an instrument is required that does not rely on consumables, is practical to use, and is robust. Designing such a modulator was the purpose behind the Masters project of Ognjen Panić.[9] However, as full characterization of the modulator was not completed, it was the focus of the research in this project. The research included: completing the robustness test, testing modulators made with thinner walled capillaries, and designing a single stage modulator. A comparison of the signal-to-noise ratio of one-dimensional gas chromatography (1D-GC) and two-dimensional gas chromatography (2D-GC) was also performed.

1.1 Comprehensive two-dimensional gas chromatography

The need for GC × GC arose from the demand for more detailed characterization of complex mixtures. In conventional gas chromatography, compounds are separated according to one major property, e.g. the vapour pressure of a compound. GC × GC allows for an additional property (e.g. polarity or chirality) to be used to separate a mixture of compounds. In addition, it provides significantly larger peak capacity. Analytes that remain unresolved from the 1D-GC process have a greater chance of being resolved by GC × GC due to the increased selectivity and peak capacity. The typical design of a GC × GC instrument is shown in Figure 1-1. It consists of an injector (a), followed by a primary column (b), a modulator (c), a secondary column (d), and

finally a detector (e). Typically, the primary column is coated with a non-polar stationary phase, and the secondary column with a polar phase.

Multi-dimensional separations are not a new concept. In the field of thin-layer chromatography (TLC), two-dimensional separations have been used for a long time to increase selectivity and increase peak capacity. In a standard TLC experiment, a sample is placed in the corner of a thin-layer plate, and the plate is placed in a solvent. After the plate has been developed and the initial separation has occurred, the plate is dried, rotated 90^{o} and developed in a different solvent to allow for an additional separation. As a result of the additional selectivity and increased peak capacity, there is a greater chance for co-eluted compounds to separate if they have not done so in the primary dimension.

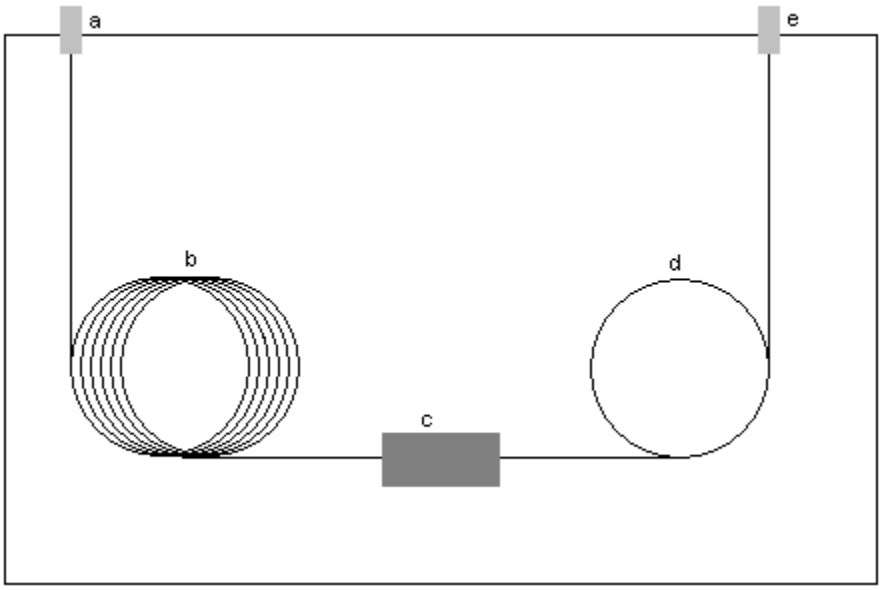

Figure 1-1 A block diagram of GC × GC system; a) Injector; b) Primary Column c) Modulator; d) Secondary Column e) Detector [10]

In order to maximize the separation power, two-dimensional gas chromatography should be comprehensive.[10,11] In other words the entire sample must be subjected to separation in two dimensions, unlike the heart-cut technique where only part of the sample undergoes the secondary separation.

Comprehensive 2D-GC requires that a modulator be placed between the primary and the secondary columns. The modulator works by periodically collecting/sampling the effluent from the first column and then re-injecting it into the secondary column. A modulation time of several seconds is typically used to allow enough time for the compounds to elute from the secondary column before the next injection cycle begins. Figure 1-2 shows what might happen if two columns were connected in a series with no modulation. Figure 1-2 (A) shows three peaks that have undergone separation provided by the first column's stationary phase. In Figure 1-2 (B), due to the change in the stationary phase in the second column from the first column, peak 2 begins to migrate through the column faster then peak 3. Peak 3 is retained in the second column more than peak 2, and this is why the change in migration occurs. Figure 1-2 (C) shows peak 1 passing peaks 2 and 3, and therefore peak 1 ultimately elutes before them. Finally, in Figure 1-2 (D), peaks 2 and 3 begin to co-elute. The stationary phase of the second column interacts with peaks 2 and 3 more strongly, whereas peak 1 passes through with little interaction. This is a good example of why a modulator is needed in GC × GC; if separation in the first column is not retained through the second column, then two-dimensional separation will not occur.

Figure 1-3 is an example of the same peaks and the same columns with modulation. Figure 1-3 (E) shows, just as in Figure 1-2, the three peaks that have undergone primary separation. Figure 1-3 (F) illustrates peak 3 being trapped by the modulator. In Figure 1-3 (G),

peak 3 is injected into the secondary column as peak 2 is trapped by the modulator. Finally, in Figure 1-3 (H), peak 2 is injected into the secondary column where secondary separation takes place. This could not occur without the modulator (see above). This example shows that by adding a modulator, the primary separation can be retained and secondary separation can occur.

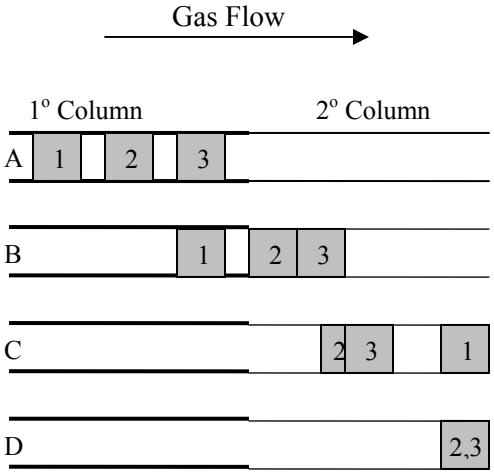

Figure 1-2: A diagram of two columns with no modulator[10]

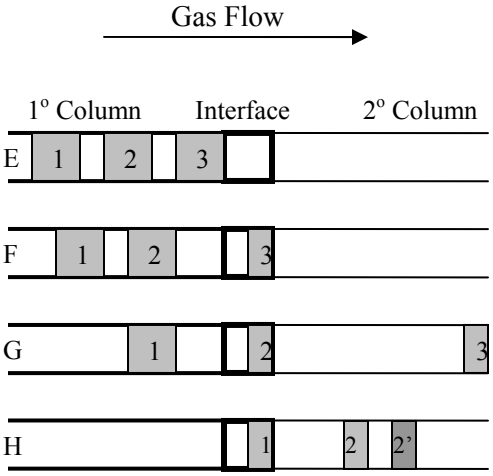

Figure 1-3: A diagram of two columns with a modulator[10]

1.2 Improvement in the Signal-to-Noise Ratio

One of the inherent problems in chromatography is peak broadening, which reduces peak capacity and decreases the signal-to-noise ratio. A trapping modulator can correct this problem; as trapping of effluent from the primary column occurs, it also recollects its components into a narrow band (See Figure 1-3 (F)). Thus, when the trapped components are re-injected into the secondary column (See Figure 1-3 (G)), the peaks are narrower and taller than they were in the primary column. This increases the signal, which in turn, improves the signal-to-noise ratio.

In addition to producing narrower analyte peaks, the modulator also increases sensitivity by separating the analytes from the chromatographic noise. The main component of noise in chromatography is column bleed caused by decomposition of the stationary phase. The bleed from the first column is modulated together with the analytes, which then elutes from the second column in dead time as it is not retained. This separation reduces the chromatographic noise, which further improves the signal-to-noise ratio.

1.3 Data Interpretation

In a GC × GC experiment, the raw data is a one dimensional representation of the two dimensional chromatogram. A computer program must thus be used to produce a two-dimensional chromatogram. The program works by taking the raw chromatogram and "cutting" it every modulation period. Each slice is then arranged side by side as depicted in Figure 1-4 (C). This arrangement is ideal for analyzing the chromatogram on a computer, as it can be viewed from any direction using appropriate computer software. This 3-D chromatogram is able to show the peak intensity, as well as the primary and secondary retention times. A topographical view of the chromatogram is an ideal representation on paper; it shows differences in peak intensity through the use of different colours. The three peaks marked with an asterisk (*) in Figure 1-4 (A) all have the same secondary retention time and only differ by the primary retention time. When the slices are arranged side by side in Figure 1-4 (C) and (D), it is clear that these three peaks originate from the same compound. By sampling a primary dimension peak three times, it helps to preserve the primary dimension separation. This means that if a modulation period is six seconds wide, the first dimension peak must be eighteen seconds wide.

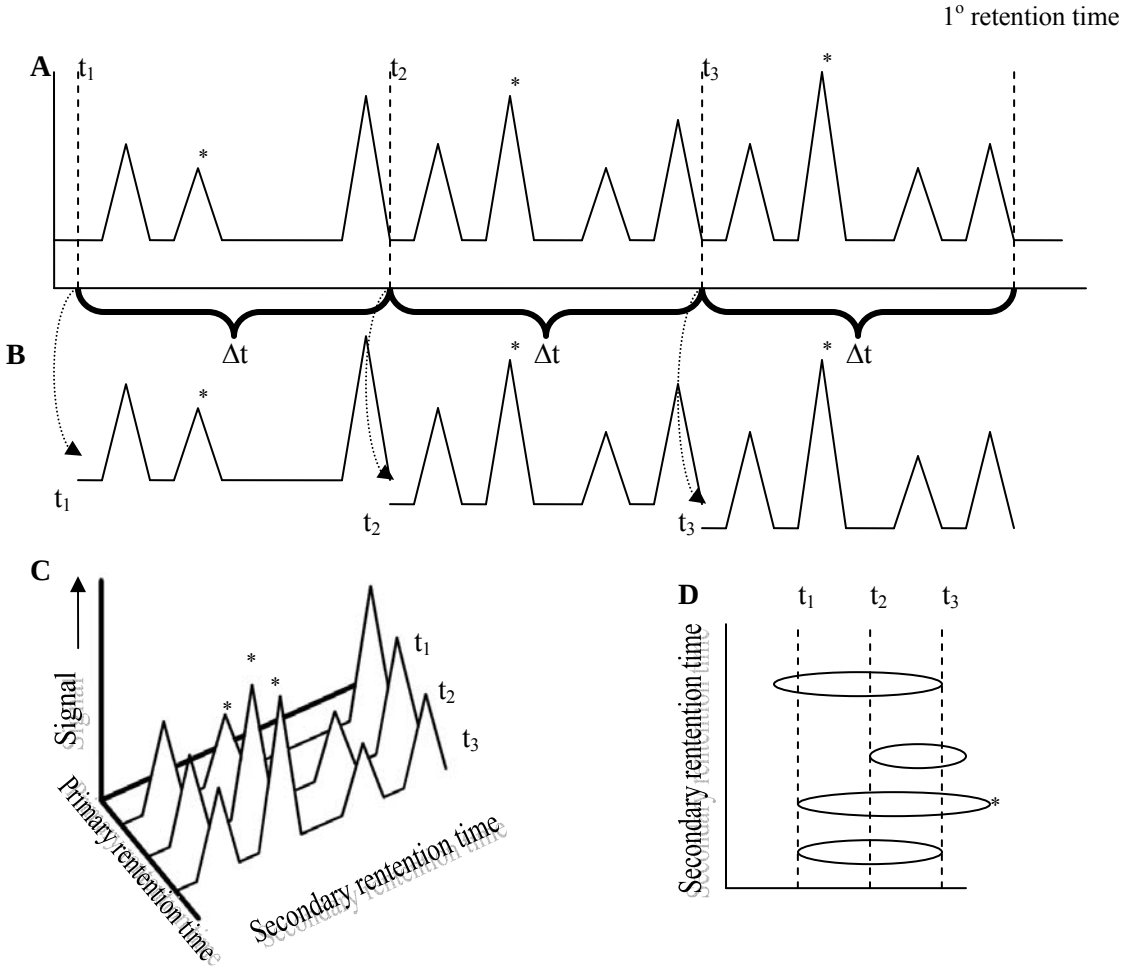

Figure 1-4: Data interpretation in GC × GC. (A) The chromatogram is recorded by the detector along with the injection times (t_1, t_2, and t_3) into the secondary column. The modulation time is represented by Δt. (B) The chromatogram is cut into individual "slices" using computer software. (C) The individual second dimension chromatograms are then aligned to produce a 3-D chromatogram.(D) A top down view of the 3-D chromatogram (based on ref.[10]).

1.4 History of GC × GC Modulators

The GC × GC modulator arose from the need to create a proper interface between the primary and secondary columns. This entailed establishing an effective way to periodically trap and re-inject analytes. Many designs have been developed over the past years to varying levels of success in an attempt to accomplish this goal. The most successful modulators were those that were the most robust and capable of generating narrow injection bands.

1.4.1 Heater Based Thermal Modulators

The first working GC × GC modulator was developed by Liu and Phillips.[12] The modulator was created using a segment of a fused silica capillary which was coated with gold paint. The modulator was placed between two GC columns. The analyte from the primary column was trapped within the stationary phase of the modulator capillary. In order for the analyte to be re-injected into the secondary column, the capillary was periodically resistively heated. This design resulted in the potential breakthrough of some peaks due to the fact that when the trapped effluent was remobilized, any analyte entering the modulator would not be collected. This caused irregularities in peak shapes. A dual-stage modulator was subsequently designed to remedy this.

The dual-stage trap, shown in Figure 1-5 (A), eliminated the breakthrough problem by trapping the effluent in two stages. The dual-stage modulator, like the single stage one, was also made of a section of fused silica capillary and coated with gold paint on the outer surface. However, the capillary was resistively heated in two sections instead of one. As a result, the analyte would first enter the modulator and become trapped. The section of the capillary between

points X and Y (Figure 1-5 (A)) would be resistively heated, remobilizing the analyte. The remobilized band, as well as any analyte entering the modulator during the desorption cycle would then be trapped in the second section of the modulator. After a predetermined amount of time, the section between Y and Z would be resistively heated, and the band would be injected into the secondary column. This second stage provided improved peak shape as a result of the elimination of breakthrough. This modulator, however, was not robust and was difficult to manufacture in a reproducible fashion.

The rotating thermal modulator, also developed by Phillips et al.,[13,14] was the first commercially available GC × GC interface. This design, as shown in Figure 1-5 (B), used a rotating heater in place of direct resistive heating of the trapping capillary. As the periodically rotating heater passed along the capillary, the trapped analyte band would be mobilized in the heated section and focused as it moved along the modulator into the secondary column. This design proved to be more robust than previous thermal modulators, though it had difficulty trapping volatiles and was impractical for high-boiling compounds due to the limited thermal stability of the stationary phase in the trapping capillary. This modulator would therefore be impractical for field work; its limited robustness and the frequent need for readjustments would act as hindrances.

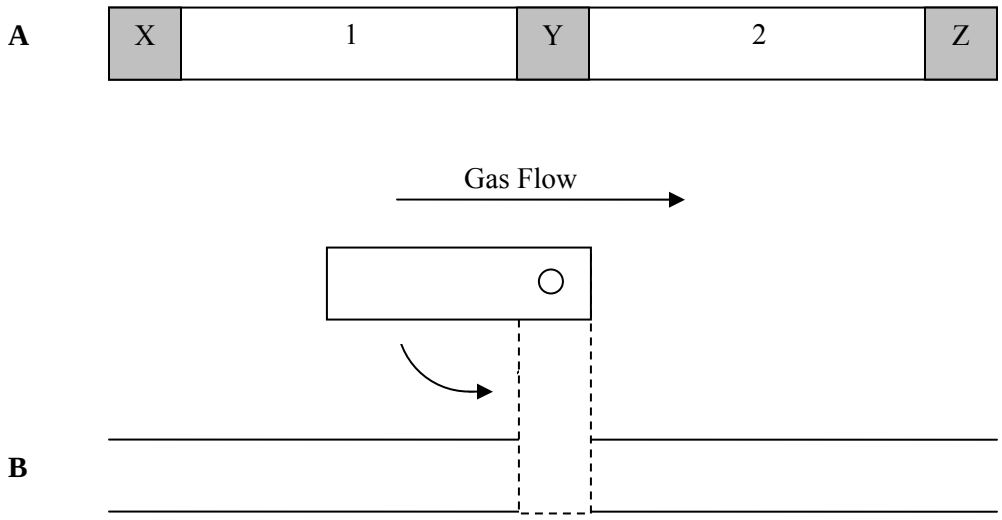

Figure 1-5: Block diagrams of the thermal based modulators designed by Phillips et al. (A) The dual-stage interface with resistive heating,[12] and (B) the rotating thermal modulator that provided approximately 100°C increase of temperature above the oven temperature.[13,14]

1.4.2 Cryogenic Based Thermal Modulators

The next step in the development of GC × GC modulators was based on cryogenic cooling. Using cryogenics allowed for analyte bands to be trapped at a temperature below the oven temperature, whereas with the rotating thermal modulator, analyte bands were trapped at the oven temperature. With the use of cryogenics, volatile compounds could be analyzed. Furthermore, as remobilization of the analyte bands could be achieved at the oven temperature, this extended the upper temperature limit of the separation to the thermal stability of the stationary phase, which allowed for the analysis of semi-volatile compounds as well.

The first cryogenic interface, called the longitudinally modulated cryogenic system (LMCS), was designed by Marriott et al.[15] The modulator (Figure 1-6) consisted of a liquid CO_2-

cooled chamber that moved back and forth between two positions along the end of the primary column. The analyte bands were first trapped when the cryogenic chamber was in the trapping position (T). The chamber then quickly moved to the release position (R), where the analyte bands that were trapped at (T) were re-collected together with any bands entering the modulator at the same time. The chamber was then moved back to the (T) position, and the bands that were trapped at the (R) position were re-injected into the secondary column.

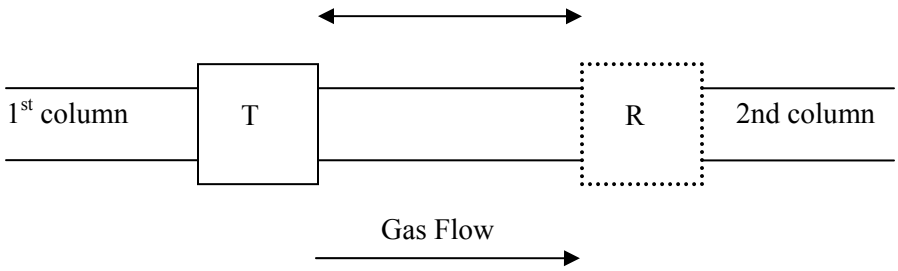

Figure 1-6: Longitudinally modulated cryogenic system (LMCS)[15]

The first cryogenic interface with no moving parts was designed by Ledford and Billesbach.[16] This model (Figure 7A) trapped the analyte bands in the modulator at two points using cold CO_2 jets (CJ_1 and CJ_2) and remobilized the bands with hot air jets (HJ_1 and HJ_2). As the analyte bands entered the modulator, they were trapped with cold CO_2 from CJ_1 (Figure 1-7 A) and then remobilized with the hot air from HJ_1. The analyte bands were trapped again by CJ_2 together with any bands entering the modulator at the same time, and re-injected into the secondary column by activating HJ_2. This design was made commercially available through Zoex Corporation and later through LECO Corporation, which replaced the CO_2 jets with liquid nitrogen-cooled gas jets.

Next, Harynuk and Górecki developed another dual-stage cryogenic modulator which was devoid of moving parts.[17] Two Silcosteel® capillaries were placed in series inside of a cryochamber, which was filled with liquid nitrogen. Analyte bands were quickly trapped when entering the modulator and then remobilized by resistively heating the capillaries in two stages.

Beens et al. designed a dual-stage cryogenic modulator that relied on the oven temperature for the remobilization of the analyte bands.[18] When analyte bands entered the modulator, they were trapped using upstream cold CO_2 jet (U) (Figure 1-7 B), and remobilized by the temperature of the oven when the jet was turned off. The bands were then re-trapped with a downstream cold CO_2 jet (D) (Figure 1-7 B), and re-injected at the oven temperature into the secondary column. This model, shown in Figure 1-7 B, has been made commercially available by the Thermo Electron Corporation.

To further simplify the cryogenic interface, Ledford et al. removed one pair of jets and added a delay loop.[19] In this design, as shown in Figure 1-7 C, the primary and the secondary columns were placed parallel to one another, and were connected with a delay loop. Analyte bands that entered the modulator were trapped by the cold nitrogen gas jet (C) (Figure 1-7 C), and were remobilized by the hot air jet (H) (Figure 1-7 C). The bands would then travel through the delay loop until they were trapped again by (C) at the second trapping position and re-injected into the secondary column by (H). This modulator is more difficult to optimize than any of the preceding models as any time chromatographic conditions such as carrier gas flow rates are changed, the length of the delay loop needs to be carefully adjusted. Harynuk and Górecki further improved upon this model by utilizing a liquid nitrogen spray instead of cold nitrogen gas.[20] With this change, very volatile analytes such as propane could effectively be trapped.

A recent development in cryogenic interfaces come from replacing liquid nitrogen with cold air in a cryogenically cooled chamber as introduced by Sacks et al.[21] The single stage unit re-mobilizes the analytes by resistively heating the trapping capillary. While this model requires little investment, it is not effective in modulating both low and high boiling compounds.

More recently Libardoni et al. improved the cryogenically cooled cold air modulator by replacing the cryogenics cooling system with a liquid cooling system[22]. This increased the range of compound that the modulator was effective at trapping, but still does not include some of the low and high boiling compounds.

As with many areas of analytical chemistry miniaturization of instrumentation is a growing interest. Kim et al. recently introduced a micro thermal modulator that utilizes micro-channels that are grown on a wafer[23]. The modulator was constantly cooled using a thermoelectric cooling device and heated periodically using micro-heaters. Though it has potential use in μGC × μGC the modulator has a limited range of compounds that it can modulate.

Although cryogenic modulators are very effective, they are far from ideal for field analysis. Cryogenic agents such as liquid nitrogen or liquid carbon dioxide would constantly need to be replenished. As field work is often undertaken in locations which might be difficult to access, daily trips to re-stock the cryogenic agents would not be practical. Bringing an entire campaign's worth of cryogenic material would also be ill advised as the sheer amount required would be unrealistic to transport. For example, the average rate of consumption of commercial liquid nitrogen modulators is 50 to 100 L/day; in a four week field campaign, 1400 to 2800 L of liquid nitrogen would be required.

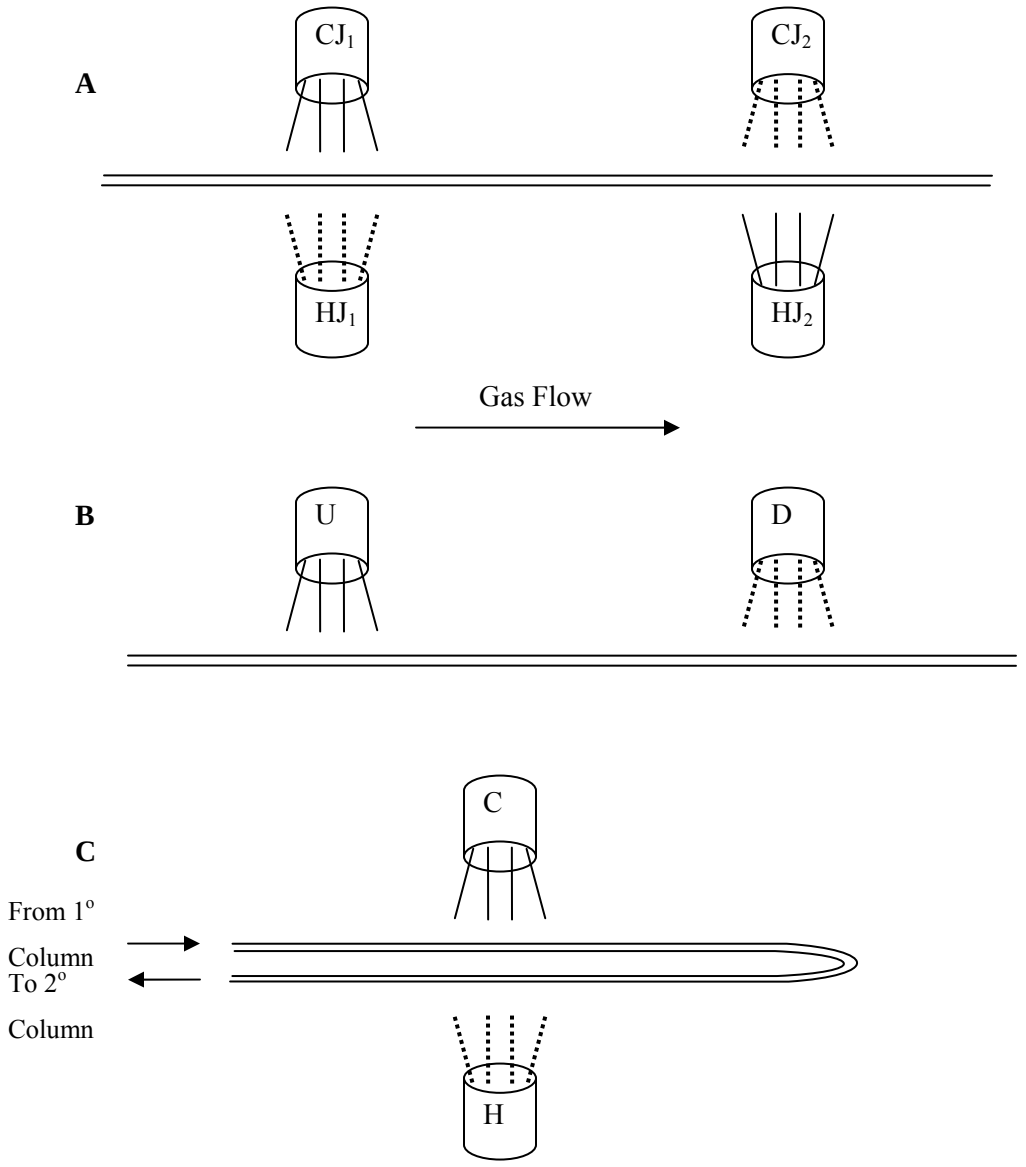

Figure 1-7: Block diagrams of dual stage cryogenic interfaces with no moving parts. (A) Alternating cryogenic jets (CJ_1 and CJ_2) for analyte trapping with hot air jets (HJ_1 and HJ_2) for re-mobilization.[16] (B) Beens' modulator using two cryojets with band remobilization at the oven temperature.[18] (C) With the addition of the delay loop, only one alternating cryogenic jet and hot jet are required.[19]

1.4.3 Valve Based Modulators

Over the years, a number of valve based modulators have been created. The first valve based interface was developed by Synovec et al. It utilized four ports of a 6-port diaphragm valve.[24] The modulator had two set positions. The first was a sampling mode in which the sample from the primary column would enter the secondary column. The second position was a venting mode in which the sample was released into the atmosphere. During the venting mode, separation would occur in the secondary column owing to an auxiliary gas supply which maintained the flow of the mobile phase in the column. This procedure would unfortunately vent 80% to 90% of the sample, which ultimately decreased sensitivity in comparison to what could be achieved with trapping GC × GC modulators. In addition, the upper operational temperature limit of the valve was rather low (~180°C), which made the analysis of semi-volatile compounds practically impossible.

Seeley et al. later designed a modulator which, with the addition of a sample loop, used all six ports of a diaphragm valve.[25] The first stage in this procedure was to fill the sample loop with the analytes. The valve would then switch, allowing the carrier gas from the auxiliary supply (delivered at a much higher pressure) to compress the analyte band collected in the loop before injecting it into the second column. With this design, approximately 80% of the sample from the primary column would enter the secondary column, which was made possible by the compression of the analyte in the sample loop.

Later, Seeley et al. solved the problem of the low temperature limit of the diaphragm valves by using two sample loops and a pneumatic switch operated at room temperature.[26] This design allowed for one loop to be filled while the contents of the other loop was injected into the

secondary column. The main disadvantage of this modulator was the very high carrier gas flow rate required to effectively flush the loops, making it incompatible with mass spectrometric detection. Also, this design only allowed for short modulation periods (up to a maximum of 2 seconds), which led to reduced peak capacity. Despite this, the modulator was successfully used in many applications.[27]

1.5 Vortex Cooler

A vortex cooler can serve as an alternative to cryogenic cooling in some applications. The only supply required for its operation is compressed air, which can be easily obtained in the field through an air compressor. The cooler separates high kinetic energy air molecules from low kinetic energy ones. When the high pressure air enters the apparatus, a vortex is formed. The high kinetic energy air molecules tend to move towards the outside of the vortex, whereas the low kinetic energy air molecules tend to travel to the inside of the vortex.[28] This allows for the high kinetic energy air molecules to be released at the top of the apparatus, leaving the low kinetic energy air molecules to be ejected from a nozzle at the bottom, where they are utilized to cool the modulator to temperatures down to about 40^{o}C below the supply gas temperature. The characteristics of a vortex blower thus make it an ideal replacement for cryogenics when used in field analysis.

Figure 1-8: Vortex cooler. Red arrows indicate high kinetic energy air molecules, while the blue arrows indicate low kinetic energy air molecules.[28]

1.6 Detectors

In comprehensive 2D GC peaks are focused by the modulator, making them narrower than in conventional GC. A detector with a fast data acquisition rate is therefore required. For a chromatographic peak area to be obtained reliably and reproducibly, a minimum of 10 data points per peak must be collected. For example, if the average peak width is 150 ms, an acquisition rate of 70 Hz must be used.[11] A flame ionization detector (FID) is commonly used in GC × GC, as it can easily provide data acquisition rates of up to 200 Hz. A mass spectrometer, commonly used as a detector in GC, is a better option, as it provides additional information about the analyte. With modern, fast scanning quadrupole mass spectrometers, a scanning rate of 10,000 amu/s can be achieved. This is still insufficient for the narrow peaks generated by GC×GC, hence such spectrometers were found suitable for only a limited number of GC × GC applications. A time-of-flight mass spectrometer (ToF-MS) better fulfills the requirements of GC

× GC because of its much faster spectral acquisition rate (up to 500 spectra/s). It is therefore the preferred choice in GC×GC – MS analysis.

In addition to chromatographic separation, deconvolution software can help identify peaks that have continued to co-elute after two-dimensional separation. This adds a third dimension of separation, which makes GC × GC-ToF MS one of the most powerful analytical techniques.

1.7 Viscosity of Gases

While the Hagen-Poiseulle equation is used to measure the pressure drop along a cylindrical tube of a fluid, it is also used to measure viscosity and how temperature affects it.[29] In the case of a gas, viscosity increases with temperature. As the viscosity increases, the flow of the gas decreases if the pressure remains unchanged. In normal gas chromatography applications, the temperature is programmed to increase at a predefined rate throughout the experiment. This requires the computer program controlling the GC to actively change the inlet pressure if the flow is to remain constant. Accordingly, if the temperature is increased rapidly and there is no compensation of the inlet pressure, the flow will effectively be stopped or at least reduced.

1.8 Previous Work

The M.Sc. project of Ognjen Panić involved the design of a thermal modulator that could be easily used in field analysis. This project started as a collaboration with Prof. Allen Goldstein of the University of California in Berkeley in order to design a modulator that could be used in

their thermal desorption aerosol two dimensional gas chromatography system (2D-TAG).[30] As the 2D-TAG was meant for field analysis of the semi-volatile fraction of air particulate matter ($PM_{2.5}$), a modulator with no moving parts or consumables was required.

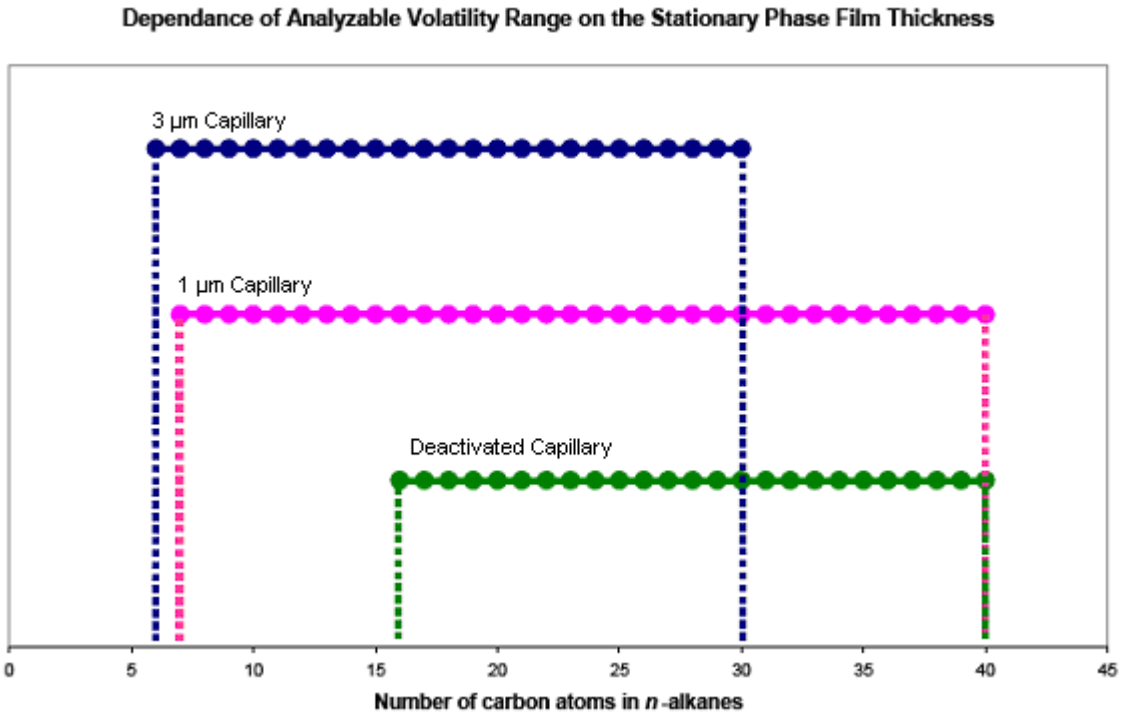

Figure 1-9: A diagram of the ranges of n-alkanes that could be effectively modulated with the traps coated with the stationary phases of different thicknesses.[9]

The modulator that Ognjen Panić developed was of a similar design to that invented by Phillips et al., but with some important modifications.[12] In particular, the fused silica capillary was replaced with a specially treated deactivated stainless steel capillary (Silcosteel®, Restek) that could be resistively heated. In addition, a cooling blower was used to aid with the trapping. When equipped with a capillary coated with 1 µm thick polydimethylsiloxane stationary phase, the modulator could effectively trap analytes in the range of volatilities of C_8 –C_{40} n-alkanes, as shown in Figure 1-9. Different stationary phase film thicknesses were also tested along with

varying temperatures of cooling air. The 3 μm stationary phase was found to be very effective in the volatile range, especially when the modulator was cooled with subambient temperature air delivered by the Vortex cooler. A bare deactivated capillary was also found to effectively trap semi-volatiles. The 1 μm stationary phase was additionally effective in trapping the analytes in the widest volatility range by utilizing cooled air at different temperatures.[9]

This newly designed modulator performed very well in comparison to other modulators in terms of peak width at half height; approximately 120 ms in the second dimension was achived.[9] Compared to other heater-based thermal modulators, this was a significant improvement. For example, Lewis et al. reported that a modulator based on a stainless steel capillary produced peak widths at half height of approximately 350 ms.[31]. A study done on the LMCS has shown peak widths at half heights of approximately 100 ms.[32] Therefore, the modulator delivered promising results both with respect to the range of analytes it could modulate and the peak widths. Overall, the performance of the new modulator was on par with many cryogenic modulators

Chapter 2
Experimental Procedure

All experiments were performed on an Agilent Technologies model 6890 gas chromatograph (Agilent Technologies, Mississauga, Ontario) with a flame ionization detector (FID). For the first dimension, a 30 m × 0.25 mm × 0.25 μm RTX-1 (Restek, Bellefonte, PA) column was utilized, while a 0.5 m × 0.25 mm × 0.25 μm ZB-50 (Zebron, Newport Beach, CA) column was used for the second dimension. The GC was also equipped with a split/splitless injector port, with hydrogen as the carrier gas. A model 7683 autoinjector (Agilent Technologies, Mississauga, Ontario) was used to inject 1 μL sample aliquots into the injector port.

The assembly of the modulator was constructed in-house with commercially available materials. The capillaries utilized in the construction of the modulator consisted of three types. The first capillary was made up of MXT-Guard 15/18 cm × 0.28 mm deactivated Silcosteel® tubing (Restek, Bellefonte, PA) with a wall thickness of 0.14 mm. The second capillary was created from MXT-1 15/18 cm × 0.28 mm × 1 μm Silcosteel® tubing (Restek, Bellefonte, PA) with a wall thickness of 0.14 mm. MXT-Guard 15/18 cm × 0.25 mm deactivated Silcosteel® tubing (Restek, Bellefonte, PA) with a wall thickness of 0.064 mm was utilized for the third capillary. Capillaries were flattened manually using two parallels and shims. In particular, three types of parallels were used in the manufacturing of the modulator, depending on the required length of the restriction. The ends of the three pairs of parallels (3/8” × 3/4” × 6”), which were purchased from KBC Tools in Kitchener, Ontario, were rounded and smoothed with a stone grinder in order to produce a gradual restriction. One pair of the parallels was left at 6”, whereas the other two were cut down to 5” and 4” lengths. All work on the parallels was completed by

the University of Waterloo's Science Technical Service (STS). Two pairs of stainless steel shims (0.005" and 0.003") were also utilized to ensure the capillaries were not over-flattened; doing so could cause fractures in the wall of the tubing. It should be noted that the thicknesses of the shims were chosen according to the outer diameter of the capillary (i.e. 0.005' with the thick walled one and 0.003" with the thin walled capillary). Subsequently, a metric micrometer (Mitutoyo, Japan) was used to measure the thickness of the flattened portion of the capillaries to ensure proper tolerance. At least a few millimeters of each end of the tubing was left unflattened to provide for enough surface area for the assembly of a ferrule-based connection to the primary and secondary columns. For the dual stage modulators, a middle contact was added by using a piece (~1 - 2 cm) of flattened Silcosteel® capillary (Restek, Bellefonte, PA) spot-welded to the modulator capillary. In some cases, one or two inches were left unflattened on one side of the capillaries in order to facilitate different experimental setups (see Chapter 3). Alligator clips with electrical leads were used to supply the electrical current to each end of the modulator via Siltite connectors (SGE, Austin, TX). A mount (Figure 2-1) designed by the group at Berkley was used to keep the modulator stationary. A hole was cut into the upper wall of the GC oven and the mount was placed on top of the oven. The mount consisted of two ceramic plates, a metal plate and a vortex cooler. A "U" shaped trough was cut into the first ceramic plate to help secure the modulator. A hole was also cut into the second ceramic plate to allow for the air from the vortex cooler to blow onto the outer wall of the modulator. A metal plate was used to provide support for the entire apparatus. A vortex cooler (Exair, Cincinnati, OH) was supplied with high pressure air (~80 psi) from an in-house supply. A flowmeter (Cole Parmer, Montreal, QC) was used to control the flow (40 L/min) of the high pressure air. The air was warmed via the GC oven using a

coiled metal tube (heat exchanger) that extended into the oven. Ferrules and nuts were used to secure the tubing system together. Interpretation of the data was obtained via the generation of GC × GC chromatograms by exporting the linear FID signals as comma-separated files (.csv). The processing of the files was done with software written in-house by James Harynuk in Matlab (Mathworks, Natick, MA).

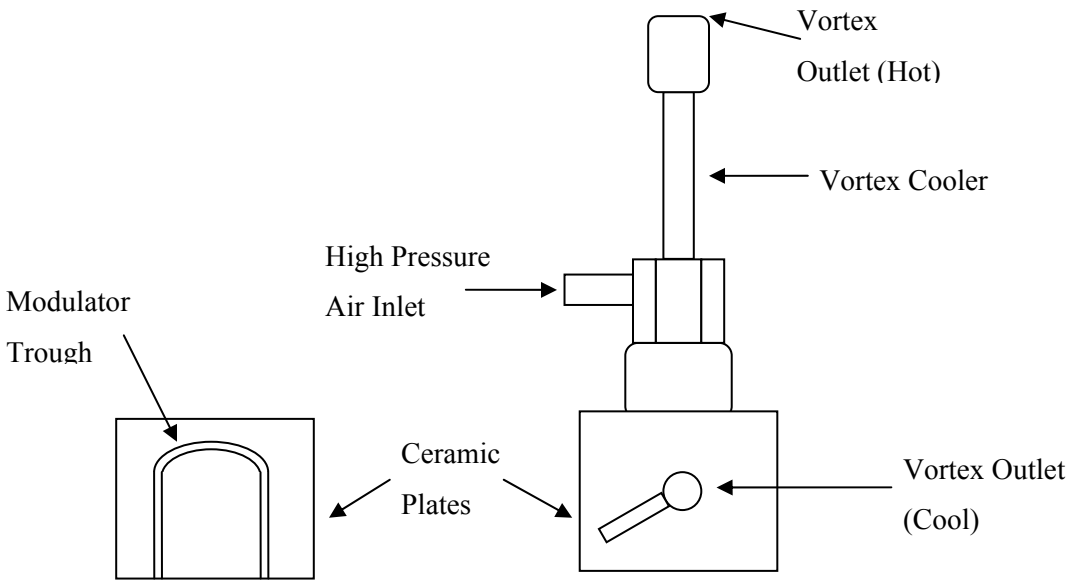

Figure 2-1: Block diagram of the modulator mount, used to secure and cool the modulator

The trapping capillaries were produced based on the procedure set out in Ognjen Panic's Masters Thesis. The procedure outlines three main steps that are required to produce the modulators. It should be noted that for the purposes of this project, some of the steps were not required depending on the particular modulator. The three steps involve flattening of the capillary, selective removal of the stationary phase, and the addition of the middle contact.

Flattening (Figure 2-2) of the capillary was required for each of the modulator models as it is essential to create a restriction in the interface (see Chapter 3). To complete this process, a capillary was placed between two parallel stainless steel shims (Figure 2-2 A) and secured with masking tape (Figure 2-2 B), which also prevented the capillary from being over flattened. The size of the shim used was dependent on the modulator being produced. Two parallels (6", 5" or 4" long) were used as an intermediate surface between the vice and the capillary (Figure 2-2 C). A vice (Figure 2-2 D) was used to ensure uniform flattening of the capillary. A micrometer was then used to check the consistency of the flattened area.

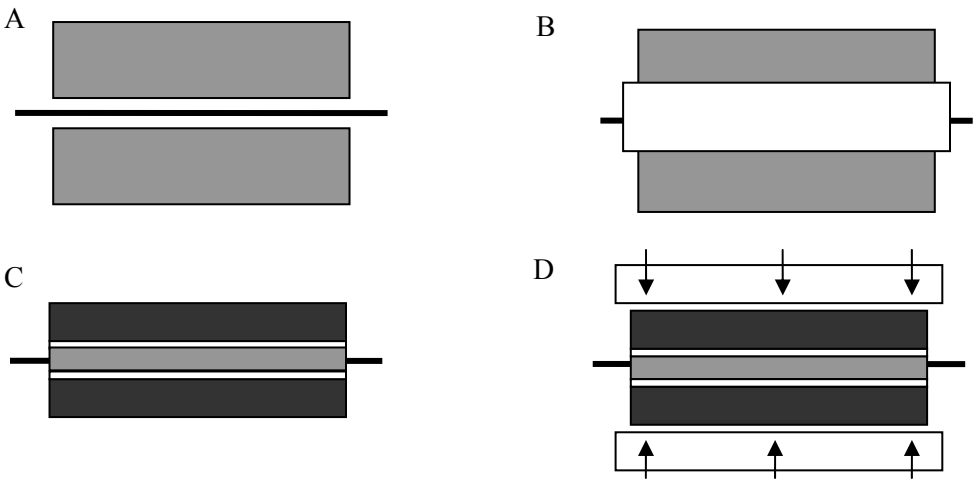

Figure 2-2: Block diagram of how to flatten capillaries in order to produce modulators. A capillary (black) is placed (A) between two shims (light grey) and then taped (white) in place (B). The apparatus from part B is then placed (C) between two parallels (dark grey), which are subsequently placed in a vice (D) where the capillary can be pressed until flattened to the proper thickness.

The second step, involving the removal of the stationary phase, is required when there is a stationary phase to remove, which depends on the capillary used (see Chapter 3). The removal

of the stationary phase is required in order to avoid problems related to cold spots. Cold spots are caused because some areas of the modulator (e.g. the vicinity of the middle connector) require more energy to warm than others, therefore might remain colder than the remainder of the capillary [9]. To remove the stationary phase, a pulsing electrical current was utilized to heat a given section of the capillary while passing high pressure air through it. The high pressure air was required to help oxidize the stationary phase. The number of pulses that were required to remove the stationary phase was dependent on the thickness of the stationary phase. For example, if the thickness of the stationary phase was 1 μm, 30 pulses would be required to remove it.

The third step involves the addition of the middle contact, which is only required for the dual stage modulator (see Figure 5-1). A piece of sacrificial flattened capillary was used as the middle contact. The capillaries were permanently connected using a spot welder. Nitrogen gas was blown over the area while it was being heated to reduce oxidation.

The resistive heating of the trapping capillaries was controlled by a capacitive discharge power supply designed and constructed by the University of Waterloo's Science Technical Services. The capacitive discharge power supply had variable voltage control and had to be calibrated for each type of trapping capillaries. Details of the calibration are given in Table 5-1. It should be noted that the power supply was originally designed for the dual-stage modulator, which is why it has two channels. Only one channel was required for the single-stage modulator. More details will be given when needed for the experimental procedure in each chapter.

Chapter 3
Comparison of Sensitivity in 1D and 2D Gas Chromatography

In addition to GC × GC with thermal modulation producing greater peak capacity than conventional gas chromatography, it also produces a greater signal-to-noise ratio. The S/N ratio was enhanced in two ways. The first and most important improvement is caused by the trapping and the reinjection of the analytes into the secondary column. The trapping of the analytes causes the compounds to be refocused so that the bands are narrower. When they are reinjected into the secondary column, the peak heights are larger, which increases the signal-to-noise ratio. The second improvement was that the column bleed noise was separated from the analytes. This effect is significant only when the temperature is high enough cause column bleed. The column bleed, which comes from the stationary phase of the primary column, is typically not retained by the stationary phase of the secondary column. This causes the column bleed to have a short retention time in the second column, which allows it to be separated from the analyte(s).

3.1 Experimental Procedure

An experimental method for 1D-GC and several methods for 2D-GC were developed. The details of the parameters are given in Table 3-1 for the subsequent analyses. There were four different experimental set ups for the 2D-GC method, which included 3 or 6 °C/min temperature program with either a 6 or 12 second modulation period.

Table 3-1: Experimental conditions for the signal-to-noise ratio experiments

Pulsed Splitless	Pulse pressure 16.8 psi until 1.00 min
Purge Flow to split vent	11.9 mL/min. at 1.00 min.
Carrier Gas	Hydrogen (5.0 UP)
Constant Flow	1.4 mL/min.
Inlet Temperature	280 °C
Initial Temperature	35 °C hold for 1 min
Temperature Program 1	To 130 °C at 20 °C/min
Temperature Program 2	To 230 °C at 3 or 6 °C/min.
Temperature Program 3	To 290 °C at 10 °C/min.
Detector Temperature	290 °C
Primary Column	RTX-1 (30 m × 0.25 mm × 0.25 μm)
Secondary Column	ZB-50 (1 m × 0.25 mm × 0.25 μm)

First, the standard solution of n-$C_{20}H_{42}$, n-$C_{22}H_{46}$ and n-$C_{24}H_{50}$ in CS_2 was analyzed using the 1D-GC method to determine the estimated detection limit (EDL)[33]. The EDL is defined as a standard with a concentration value that corresponds to an instrument signal-to-noise in the range of 2.5 to 5. After analyzing the standards, it was found that the EDL for the 1D-GC method was 10 μg/L. Once the EDL was determined, a concentration one to five times greater was used to determine the limit of detection (LOD). The determination of the LOD required injection of eight replicate aliquots of the same standard to obtain the standard deviation for the set. This was then used to determine the LOD based on peak heights. The LOD was determined using the following equation:

$$LOD = t_{n-1,\ 1-\alpha=0.99} \times s$$

t = the student's t for 99% confidence level

s = standard deviation

$n-1$ = degrees of freedom

3.2 Results and Discussion

The same procedure was applied to the 2D-GC method and it was found that the EDL was 1 µg/L. The data processing used for the 1D-GC method was then applied to the 2D-GC method to determine its LOD. The LOD's for all techniques are listed in Table 3-2. For all four experiments, with the exception of n-C_{20} and the n-C_{22} in the 6 s modulation with 3 °C/min temperature program, the 2D-GC results proved to be at least an order of magnitude better.

Table 3-2: LODs (µg/L) for each of the experiments (1D and 2D)

Analyte	LODs (µg/L)				
	1D	6 s modulation 3 °C/min	12 s modulation 3 °C/min	6 s modulation 6 °C/min	12 s modulation 6 °C/min
n-C20	87	9.3	4.4	8.2	5.2
n-C22	68	7.6	5.8	5.5	4.4
n-C24	153	14	11	12	9.9

Differences in the peak shapes of the 1D-GC experiments and the 2D-GC experiments are most relevant with respect to the improvements in the signal-to-noise ratio. The n-C_{24} peak in the 1 dimensional run is shown in Figure 3-1, while the 2 dimensional run is shown in Figure 3-3. The peaks in 2D-GC experiments were much narrower than those in 1D-GC experiments, making them much easier to detect. This was also true for the other 2 dimensional experiments

shown in Figure 3-2, Figure 3-4, and Figure 3-5, as the peaks were also much narrower and easier to detect.

In addition to the improvements in the peak shape, the peaks were being separated from the column bleed. This was most evident with Figure 3-3 and Figure 3-5 as the column bleed was at the highest levels around the C_{24} peak. In these figures the column bleed noise peaks were larger than the C_{24} peak itself.

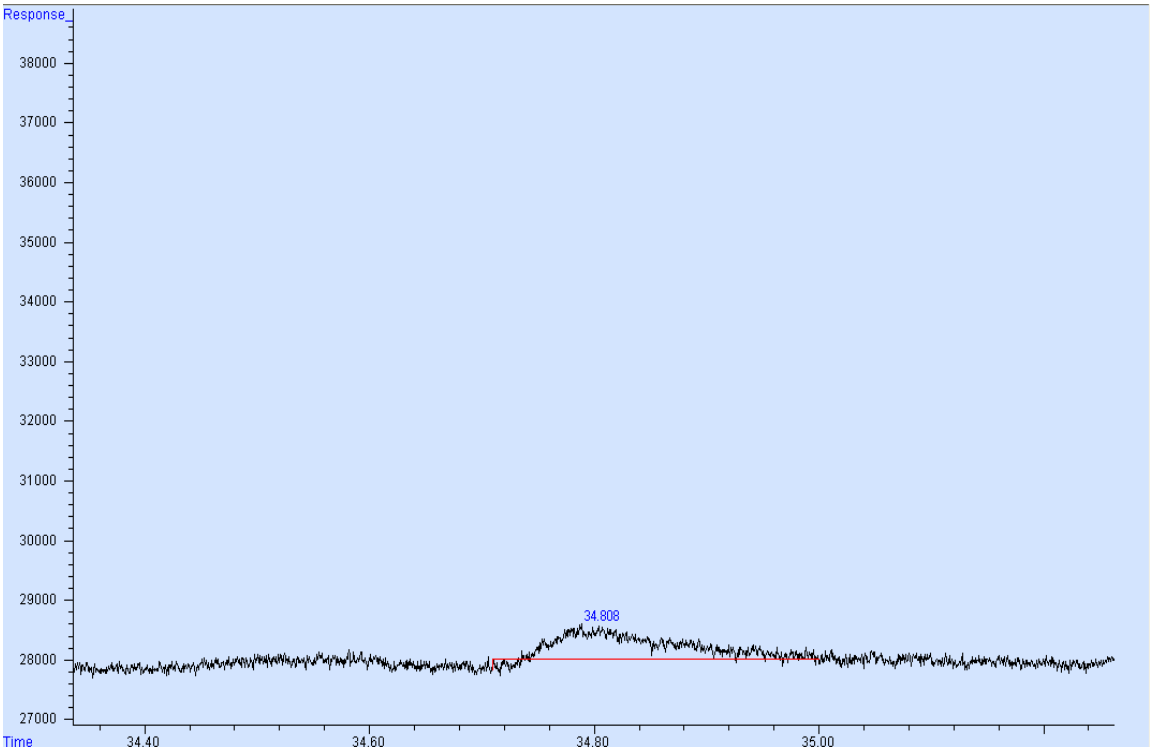

Figure 3-1: A fragment of a 1D gas chromatogram of an alkane mixture showing the n-C_{24} peak (150 ug/L) with a temperature program of 3 °C/min.

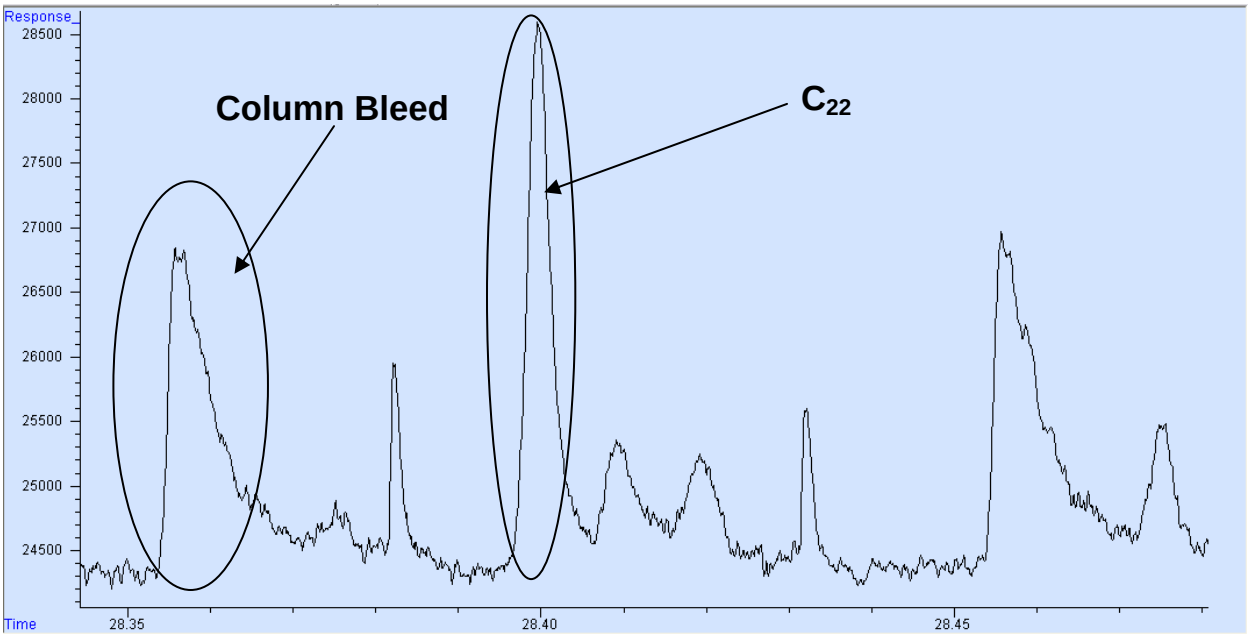

Figure 3-2: A fragment of a 2D gas chromatogram of an alkane mixture showing the n-C_{22} peak (8.5 µg/L) with a temperature program of 3 °C/min and a modulation period of six seconds.

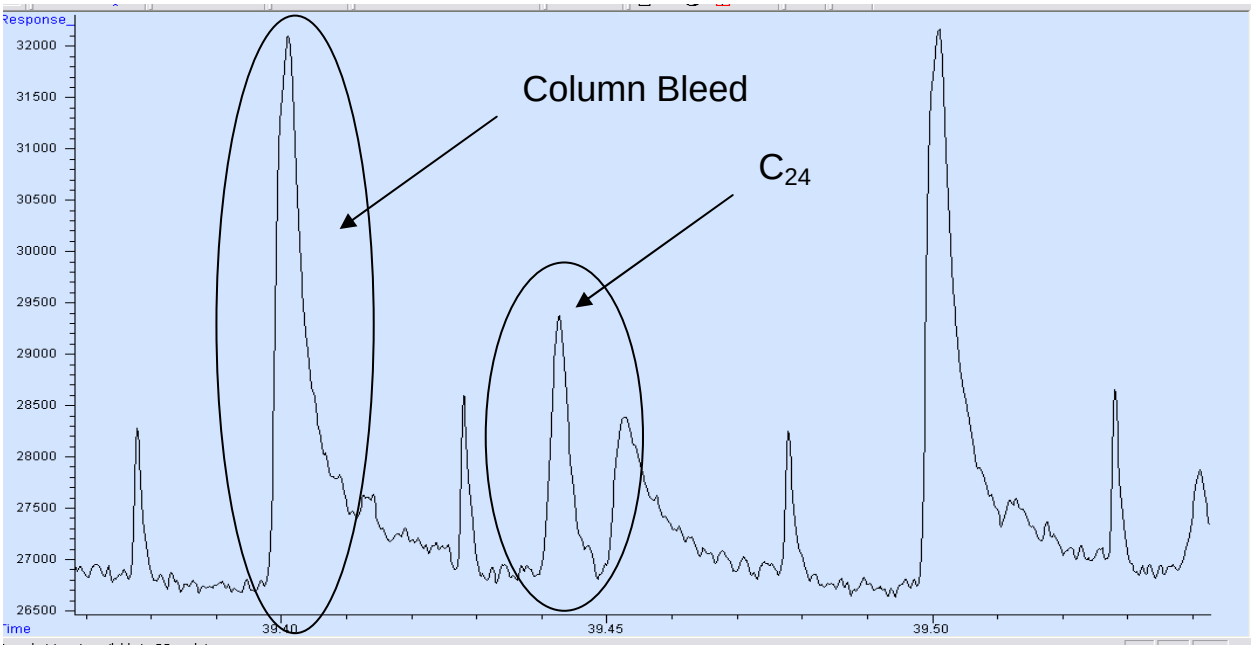

Figure 3-3: A fragment of a 2D gas chromatogram of an alkane mixture showing the n-C_{24} peak (11 µg/L) with a temperature program of 3 °C/min and a modulation period of six seconds.

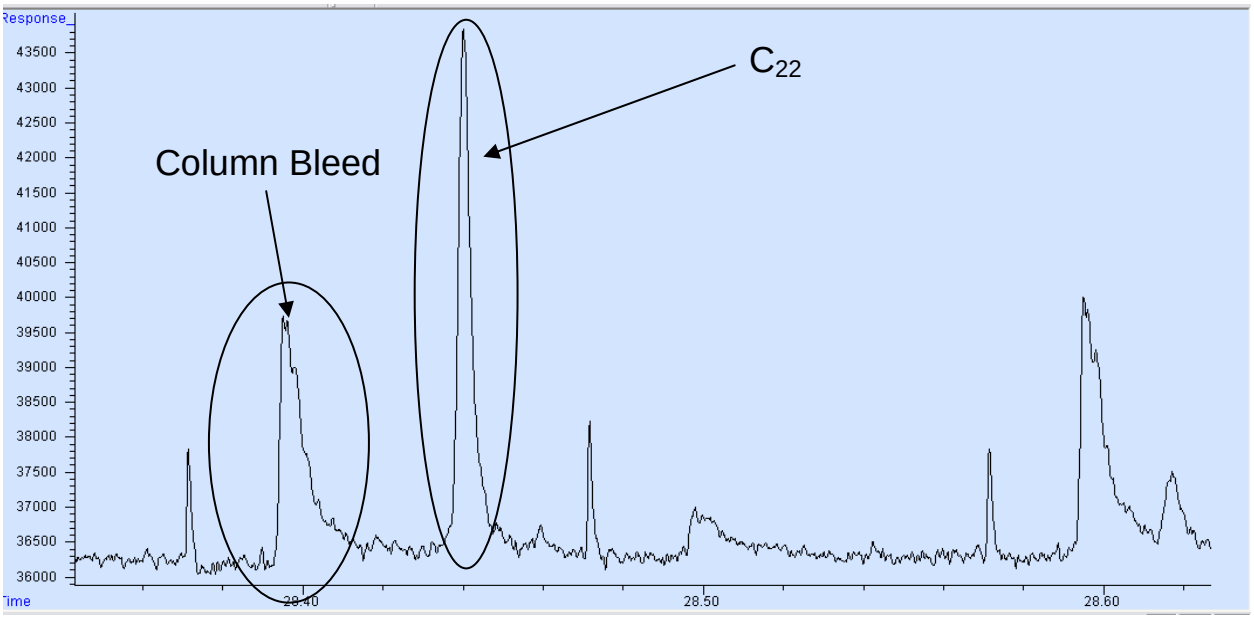

Figure 3-4: A fragment of a 2D gas chromatogram of an alkane mixture showing the n-C_{22} peak (8.5 µg/L) with a temperature program of 3 °C/min and a modulation period of 12 seconds.

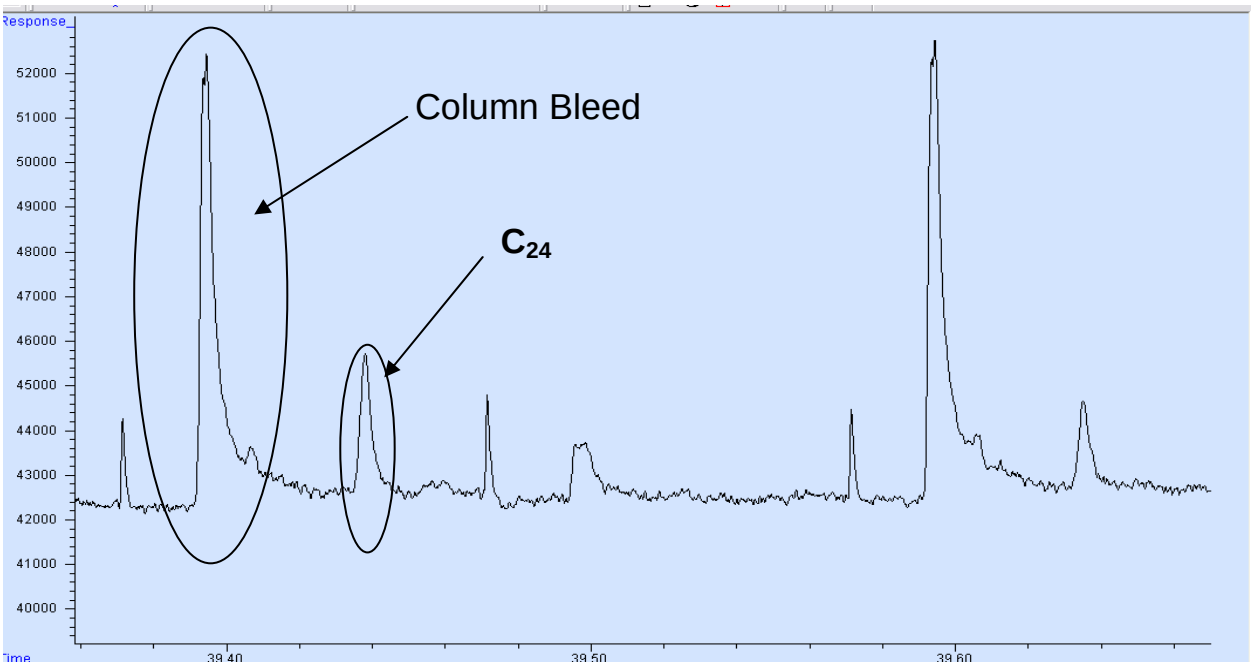

Figure 3-5: A fragment of a 2D gas chromatogram of an alkane mixture showing the n-C_{24} peak (11 µg/L) with a temperature program of 3 °C/min and a modulation period of 12 seconds.

Overall, the improvement in the single-to-noise ratio from 1D-GC to 2D-GC was about one order of magnitude. This was largely due to the refocusing of the analytes in the modulator, but there was also additional improvement in later eluting compounds because of the separation from the column bleed. This shows that 2D-GC can be a more sensitive technique than conventional 1D-GC techniques.

Chapter 4
Robustness of a Dual Stage Modulator

A key component of the evaluation of the dual-stage modulator, which was developed during the Master's project of Ognjen Panic, was the robustness test. The robustness of the modulator had to be evaluated in order to ensure it could continuously work during field expeditions.

The main issue with the dual-stage modulator's robustness was the middle contact. The first problem with the middle contact was attaching it to body of the modulator. While spot welding the middle contact to the body of the modulator rapid oxidation could occur, usually following the occurrence of a bright spark. The oxidation could lead to several possible outcomes. In some cases, a small crater or a hole in the capillary were produced. A hole rendered the modulator immediately unusable, while a crater could open into a hole over time, as the discharge through the modulator caused it to deform periodically. Even without a hole or a crater, oxidation could cause poor attachment of the middle contact. Over time, the repetitive movement of the modulator would then cause the contact to detach from the body of the modulator.

In order to combat the degradation of the modulator two improvements were done. The first was to blow nitrogen gas over the area that was being spot welded to prevent oxidation of the column wall. Under this new condition two improvements were observed. Firstly, the bright sparks were no longer observed, which would indicate that the oxidation was not occurring. Secondly, when the column wall was inspected via 10x magnification, there were no craters or holes found. The second improvement was the introduction of a new mount that was better suited

to holding the modulator in place. The new mount used screws to hold the modulator firmly, which meant that the vibrations caused by the electrical discharge would be dampened. In order to confirm that the modulator would be robust under these new conditions, a robustness test was preformed.

The robustness test was carried out over a two month period. The modulator was placed in the new mount and the discharge event occurred with a period of four seconds. The modulator was inspected daily for any breakdown in the column wall. During this period no issues were found. After the two month period was over, the modulator was removed from the mount and was inspected closely. No issues were uncovered during this time. Though no chromatograms were produced during this time, Prof. Goldstein's group from the University of California at Berkeley preformed their own robustness test while doing field studies. They found that typically the modulator was performing well for three to four weeks before a replacement was required. Overall, the modulator performed quite well under laboratory conditions, but was less than perfect for continuous use in the field. The main fault that was occurring was the middle contacted detaching from the body of the modulator.

In order to improve the connection of the middle contact a different method of attachment was attempted. The original spot welding method was replaced with silver solder. Use of the silver solder did improve the connection of middle contact to the body of the modulator. However, the heat required to melt the solder would sometimes cause the stainless steel to become brittle, which would decrease the robustness of the modulator. Though further investigation into the soldering of the middle contact may have led to a robust modulator, this study was abandoned for a more promising one, which will be the focus of Chapter 5.

Chapter 5
Design of a Single Stage Modulator

Dual stage modulators (Figure 5-1 A) were developed in order to solve the problem of analyte breakthrough which occurs when the modulator is in the desorption stage and is momentarily brought to higher temperature. During the desorption stage, the modulator is unable to trap the components of the effluent leaving the first column before they enter the second column. In contrast, a dual stage modulator is heated and cooled in two stages, which ensures that all effluent is trapped before entering the second column. Although dual stage modulators resolve the breakthrough problem, their design is more complicated; complex design, in turn, results in reduced robustness and a greater likelihood of premature failure.

An example of when a complication might occur during the manufacturing of the dual stage modulator is when spot welding is completed to attach the middle contact to the body of the modulator. In spite of controlled settings, spot welding would, on occasion, produce a hole in the modulator tubing. Furthermore, even when the spot welding process was able to produce a good contact and no holes, the periodic mechanical motion caused by the electrical discharge through the modulator would still periodically cause the middle contact to detach from the body of the modulator, rendering it inoperational.

A single stage modulator based on the dual stage modulator developed by Ognjen Panic was developed in order to overcome the problems of limited robustness and premature failure (Figure 5-1B). The key to the implementation of the single stage concept without the problem of breakthrough was to create a significant restriction to the carrier gas flow in the modulator during analyte desorption. This restriction occurs due to the fact that viscosity of gases increases

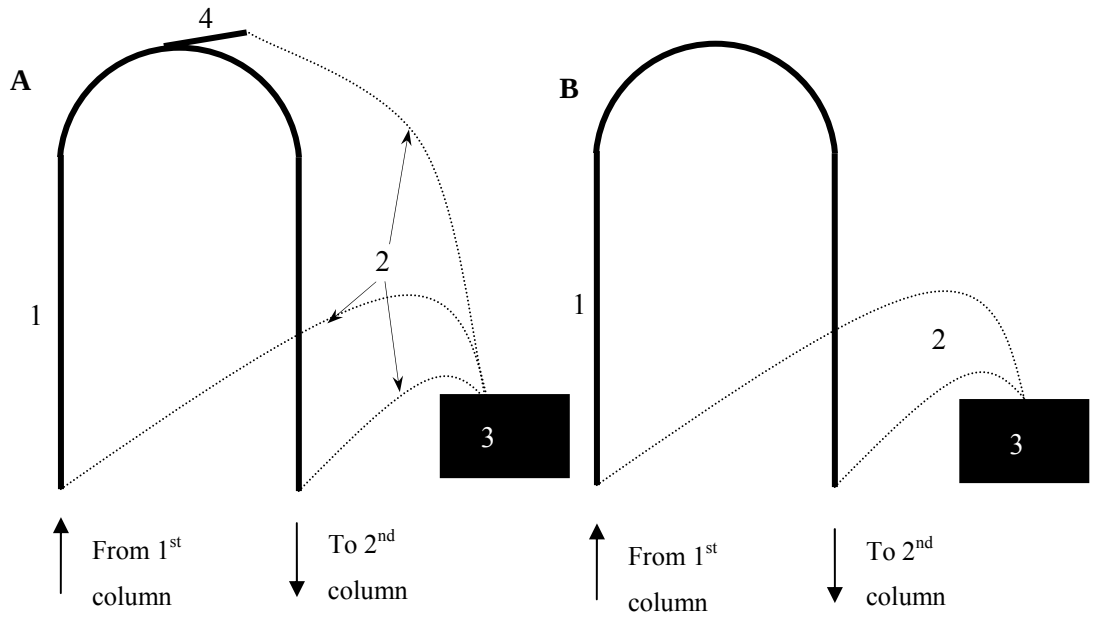

Figure 5-1: Schematic diagrams of the modulators. A: dual stage; B: single stage. 1) modulator tubing; 2) electrical leads; 3) power supply; 4) middle contact**.**

with temperature. The modulator therefore becomes a temperature-tunable restrictor. When the modulator is in the collection stage, the system is kept at a low temperature during which the carrier gas flows through the modulator with little pressure drop. In contrast, when the modulator is in the high temperature desorption phase, the pressure drop increases significantly. This pressure drop acts to impede the flow of the carrier gas. In addition to the increased pressure drop, a pressure pulse created by the rapid heating of the modulator capillary momentarily stops the flow of the carrier gas from the first column. Both the increased pressure drop and the pressure pulse reduce the risk of the analyte breaking through during the desorption stage. As a result, the single stage modulator performs almost on par with the dual stage modulator without the need for the middle contact. This makes the single stage modulator more robust and decreases the chances of premature failure.

5.1 Experimental Procedure

In order to understand why analyte breakthrough was not observed in the single stage modulator, the drop in flow caused by the increase in temperature needed to be assessed. An experiment was designed in order to determine how temperature affected the flow rate. Figure 5-2 illustrates how the experiment was set up to determine the flow of the carrier gas at different temperatures. To begin, a short piece of fused silica tubing connected the inlet (A) to the modulator (B). The modulator (B) was placed in the oven (D) in order to control its temperature. Then at the other end of the modulator (B), another short piece of tubing was connected to a flowmeter (C). The two short pieces of tubing that were used to connect the modulator (B) to the inlet and the flowmeter had internal diameters of 0.53 mm, which helped reduce the restriction. A constant pressure of 0.5 psi was used at the inlet. Temperatures were input manually and measurements were taken once equilibrium was reached.

The power supply that was used for the dual-stage modulator was also utilized for the single-stage modulator with minor modifications (i.e. only one channel was used for discharging). A temperature of approximately 350 ^{o}C was required to remobilize the analytes. An oscilloscope was utilized, along with a 50 μm K-type thermocouple which was spot welded to the capillary to determine the voltage required to heat the modulator. A temperature of 350 ^{o}C was required as shown in Table 5-1. This table further outlines the required voltage for situations when forced cooling was/was not used, as well as for each type of modulator that was tested. A list the modulators is given in Table 5-2, which includes the length of the flattened portion of the modulator, total length of the modulator, wall thickness, and stationary phase. The experimental conditions shown in Table 5-3 detail both the n-alkane and diesel experiments.

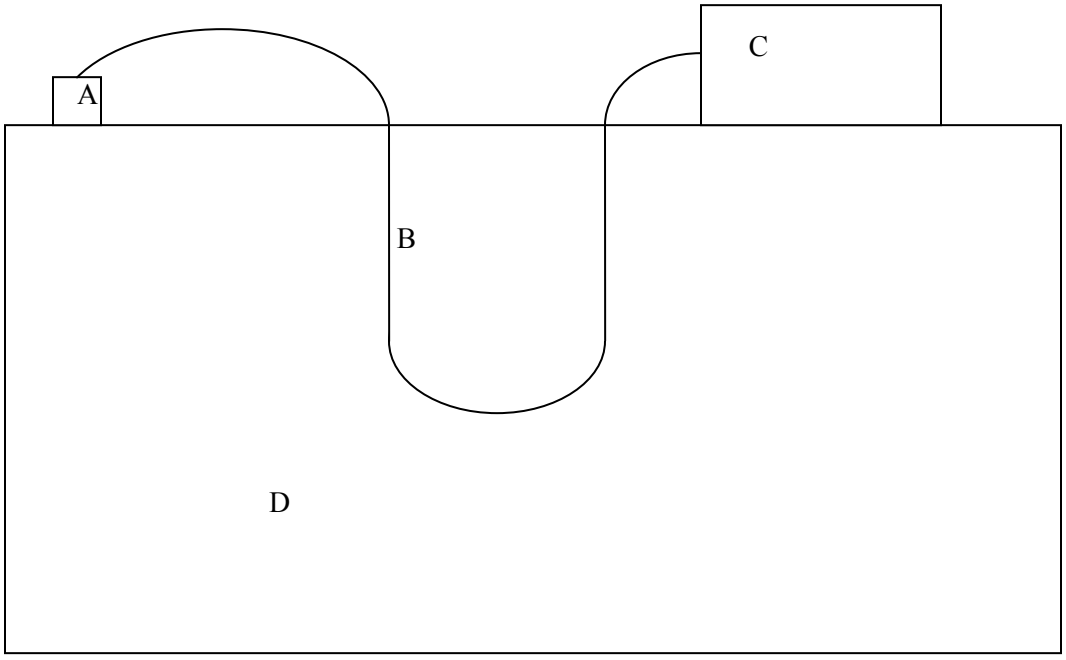

Figure 5-2: Experimental setup for flow rate of the modulator: A inlet, B modulator, C flowmeter, D oven.

Table 5-1: List of the required voltages for each of the modulator types

Modulator Type	Thick Wall 6”	Thick Wall 7”
Voltage required for 350 ^{o}C (No Vortex)	62.3 V	71.3 V
Voltage required for 350 ^{o}C (With Vortex)	66.9 V	72.9 V
Modulator Type	Thin Wall 6”	Thin Wall 7”
Voltage required for 350 ^{o}C (No Vortex)	50.5 V	57.4 V
Voltage required for 350 ^{o}C (With Vortex)	56.0 V	58.9 V

Table 5-2: List of modulators and their dimensions

Modulator Types	Length of Flatten Portion of Modulator	Total Length of Modulator	Wall Thickness	Stationary Phase
CM66	6”	6”	0.14 mm	MXT-Guard
CM56	5”	6”	0.14 mm	MXT-Guard
CM46	4”	6”	0.14 mm	MXT-Guard
CM67	6”	7”	0.14 mm	MXT-Guard
CMt66	6”	6”	0.064 mm	MXT-Guard
CMt67	6”	7”	0.064 mm	MXT-Guard
CMS66	6”	6”	0.14 mm	1 μm (PDMS)
CMS67	6”	7”	0.14 mm	1 μm (PDMS)

Table 5-3: Experimental conditions for the n-alkane mixture and diesel experiments.

Experimental Conditions	n-alkane mixture	Diesel
Initial temperature (^{o}C)	140	30
Final temperature (^{o}C)	250	250
Hold time (minutes)	0	10
Temperature ramp (^{o}C/min)	3	6
Flow rate (mL/min)	1.2	2.4
Split ratio	10:1	30:1
Injector temperature (^{o}C)	280	280
Detector temperature (^{o}C)	290	290
Carrier gas	Hydrogen	Hydrogen
Primary Column	RTX-1 (30 m × 0.25 mm × 0.25 μm)	
Secondary Column	ZB-50 (0.5 m × 0.25 mm × 0.25 μm	

5.2 Results and Discussion

The experiments were run three times and the results were averaged. Figure 5-3 A shows the results obtained. The flow at 350 ^{o}C was the most relevant due to the fact that when the modulator was in the desorption phase of its cycle, its temperature was ~350 ^{o}C. The rapid heating of the modulator tubing from around room temperature to 350 ^{o}C caused a drop in flow by about a factor of seven (7.21 mL/min at 50 ^{o}C to 1.07 mL/min at 350 ^{o}C). A comparison with theoretical results (Figure 5-3 B) obtained using a flow calculator (Hewlett-Packard) for an open capillary tube of equivalent pneumatic resistance at 350^{o}C showed that the difference in flow between the two was about a factor six at this temperature (6.41 mL/min compared to 1.07 mL/min, respectively). This drop in flow, along with the pressure pulse that was created by the rapid heating of the gas, can explain why analyte breakthrough was minimized in the restricted modulator.

The performance of the different modulators was examined using a standard solution of n-$C_{16}H_{34}$, n-$C_{20}H_{42}$ and n-$C_{24}H_{50}$ in CS_2. In order to obtain the desired peak width at half height, three variables were tested: length of the restriction, length of the open tube, and thickness of the wall. An increase in the length of the restriction should decrease the peak widths at half height, as should the length of the entire modulator (length of the open tube). A thinner wall should allow faster cooling, thus enabling shorter modulation periods.

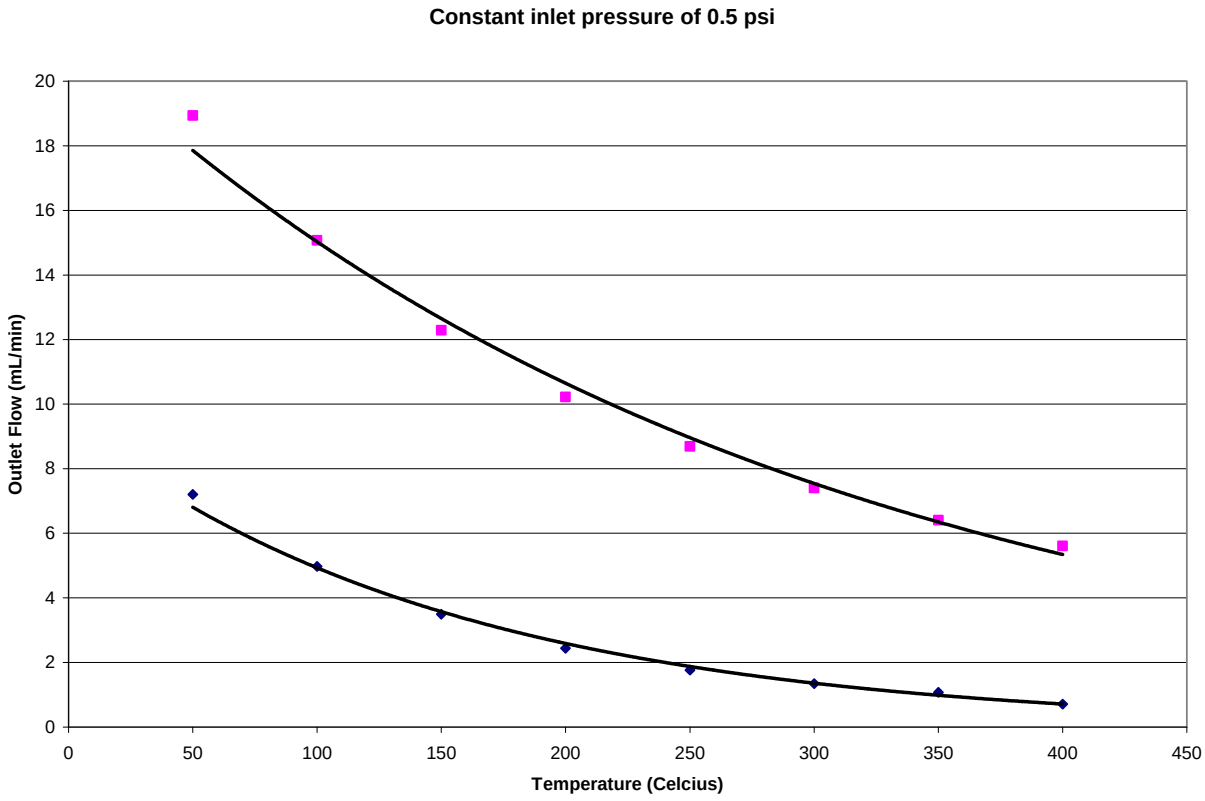

Figure 5-3: Experimental results for carrier gas flow rate through the modulator as temperature increased at a constant inlet pressure of 0.5 psi. A: results for the restricted modulator; B: theoretical results for an unrestricted modulator.

In general, as the restriction of the modulator decreased, the peak widths at half height increased. In addition, as the peak width increased, the peak shape became worse, with more pronounced tailing. In the case of the modulators with the shortest restriction (CM56 and CM46), the n-C_{24} peak (Table 5-4) was not being trapped properly, hence the width could not be determined. The average peak widths at half height for the n-C_{16} peak for the CM66, CM56 and CM46 modulators were 149, 163 and 191 ms, respectively. This shows that the peak widths at half height were increasing with decreasing restriction. Furthermore, the average peak widths at half height of the n-C_{20} peak for the CM66, CM56 and CM46 modulators were 197, 240 and 440

ms, respectively. The increase of the peak widths was much more prominent in this case. A segment was added to front end of the modulator (primary column side) that was not flattened. This was used to create an area in which a higher volume of gas was being heated. It was hypothesized that the pressure pulse created during the heating pulse would force the carrier gas through either end of the volume, but since one side had a higher restriction (due to the flattening of the capillary and increased viscosity), the gas would be forced mainly in the opposite direction of the carrier gas flow. This could potentially momentarily stop the carrier gas flow, helping prevent breakthrough.

When the restriction was held constant but the length of the unflattened portion of the modulator was increased, as evident in the case of CM66 and CM67, the peak widths at half height decreased overall. The average peak widths at half height for the n-C_{16} peak for the CM66 and CM67 modulators were 149 and 125 ms respectively. Also the average peak widths at half height for the n-C_{20} peak for the CM66 and CM67 modulators were 197 and 169 ms respectively. Finally the average peak widths at half height for the n-C_{24} peak for the CM66 and CM67 modulators were 210 and 180 ms respectively. This is a consistent improvement for all three peaks with the increase of the open tubular portion of the modulator. The average peak widths at half height for the n-C_{16} peak for the CMt66 and CMt67 modulators were 129 and 113 ms respectively. Also, the average peak widths at half height for the n-C_{20} peak for the CMt66 and CMt67 modulators were 167 and 153 ms respectively. Finally, the average peak widths at half height for the n-C_{24} peak for the CMt66 and CMt67 modulators were 184 and 201 ms, respectively. The difference between these peaks was not significant because the standard deviations were 7 and 9 ms, respectively. The improvement in the CMt67 over the CMt66 was not as significant as the CM modulators. In the case of the n-C_{24} peak, there was no significant

improvement. Overall, a perceptible pattern was evident showing that a decrease in the peak width at half height correlated with an increase in the length of the unflattened portion of the capillary. This was shown for a third time when comparing the CMS66 and CMS67 modulators (Table 5) as the n-C_8 (136 and 118 ms respectively) peak and the n-C_9 (156 and 146 ms respectively) peak both showed improved peak widths at half height. However, for the CMS66 and CMS67 modulators, the n-C_{10} (180 and 204 ms respectively), n-C_{11} (186 and 195 ms respectively), n-C_{12} (196 and 210 ms respectively) and n-C_{13} (207 and 215 ms respectively) peaks there was no significant improvement with the increase in the length of the unflattened portion of the capillary. In conclusion, the length of the open tubular portion was not as significant to the peak widths at half height as the length of the restriction itself.

When comparing the wall thickness of the modulators, the CMt (0.064 mm thick) models showed a decrease in the peak widths at half height in every case, more so than the CM (0.16 mm thick) models. First, in comparing the CM66 and CMt66 modulators, the n-C_{16} (149 and 129 ms respectively), n-C_{20} (197 and 167 ms respectively) and n-C_{24} (210 and 184 ms respectively) peaks showed a significant improvement in the peak widths at half height. Also, the comparison of the CM67 and CMt67 for the n-C_{16} (125 and 113 ms respectively), n-C_{20} (169 and 153 ms respectively) and n-C_{24} (180 and 201 ms respectively) peaks showed that there was no significant improvement in the peak widths at half height, as the standard deviations for these peaks were significant. Overall, there was evidence that some improvement in the peak widths at half height was achieved by decreasing the wall thickness of the modulator. The improvements, however, were not as significant as those associated with the length of the restriction of the modulator. In addition to the effects on the peak widths at half height, there was also an effect on the modulation period. The nature of the thin walled capillaries acts to reduce the amount of time it

takes for the modulator to return to room temperature. This can, in turn, reduce the modulation period. The shortest modulation period that was used with the thick walled modulator was six seconds. With the thin walled tubing, modulation periods could be reduced to a minimum of two seconds for short periods of time; however, the power supply could not support the rapid discharge cycle required for more regular use as it would fail prematurely. The power supply could, however, support a four second modulation period for extended periods of time.

Table 5-4: Peak width at half heights for each modulator type with deactivated stationary phase

Modulator Type	Peak width at half height in ms (1 stdev)		
	n-C_{16}	n-C_{20}	n-C_{24}
CM66	149 (3)	197 (6)	210 (8)
CM56	163 (5)	240 (10)	N/A
CM46	191 (7)	440 (40)	N/A
CM67	125 (3)	169 (7)	180 (10)
CMt66	129 (4)	167 (4)	184 (7)
CMt67	113 (2)	153 (3)	201 (9)

Table 5-5: Peak width at half heights for each modulator type with stationary phase

Modulator Type	Peak width at half height in ms (1 stdev)					
	n-C_8	n-C_9	n-C_{10}	n-C_{11}	n-C_{12}	n-C_{13}
CMS66	135 (4)	156 (3)	180 (10)	186 (6)	196 (7)	207 (7)
CMS67	118 (4)	146 (3)	204 (9)	195 (9)	210 (6)	215 (6)

In order to further characterize each of the successful modulators, a sample of diesel fuel was obtained from the University of Waterloo's gas station. A more complex sample (i.e. diesel) was required to ensure that a true two-dimensional separation was being achieved. When

comparing the CM66 (Figure 5-5) and CM67 (Figure 5-6) modulators, both experiments showed very good separation with consistently narrow peaks throughout the entire run. The CM67 modulator produced peaks with less tailing compared to the CM66 modulator, but overall, the results were comparable. This can be seen more clearly in the three dimensional plots in Figure 5-11 (CM66 modulator) and in Figure 5-12 (CM67 modulator), where somewhat more tailing could be seen for the CM66 modulator compared to the CM67 modulator. However, when comparing the CMt66 (Figure 5-7) modulator to the CMt67 modulator (Figure 5-8), greater differences were evident. Furthermore, there was improvement in the peak shape in the CMt67 model over the CMt66 model. When comparing the CMS66 (Figure 5-9) modulator and the CMS67 (Figure 5-10) modulator the same trend continued. The CMS67 modulator produced peaks with less tailing than that of the CMS66 modulator. Again, when comparing the three dimensional view of the CMS66 (Figure 5-15) modulator and the CMS67 (Figure 5-16) modulator chromatograms, it is clear there was less tailing produced from the CMS67 modulator.

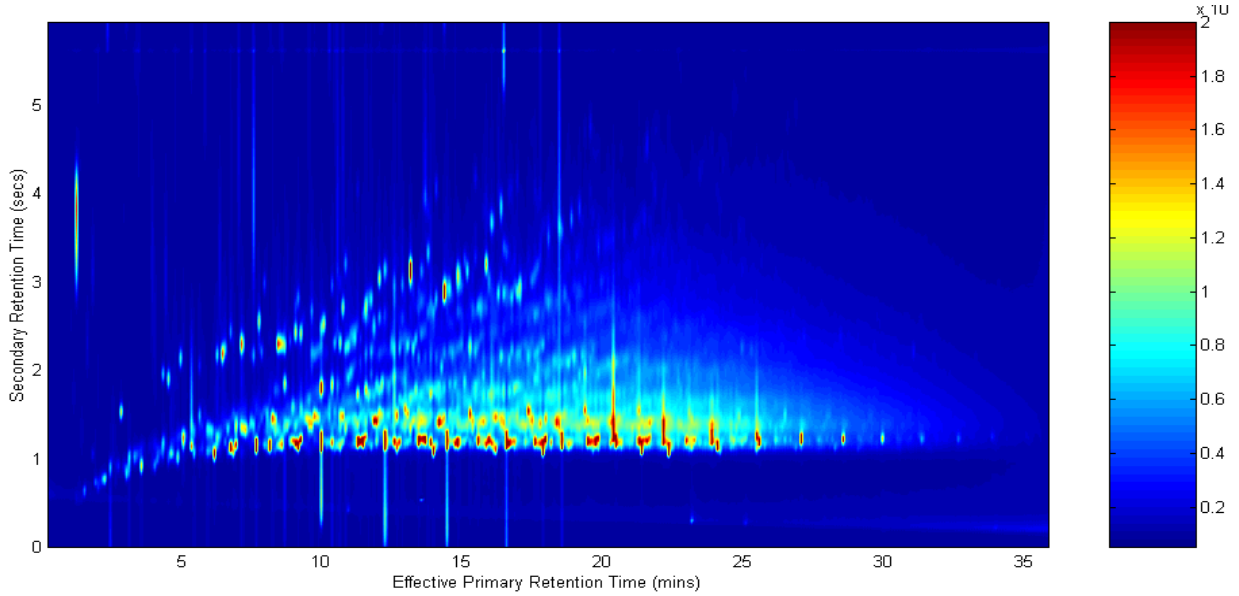

Figure 5-4: A two-dimensional chromatogram of a solution of diesel fuel in CS_2 (1:10 dilution) using CM66.

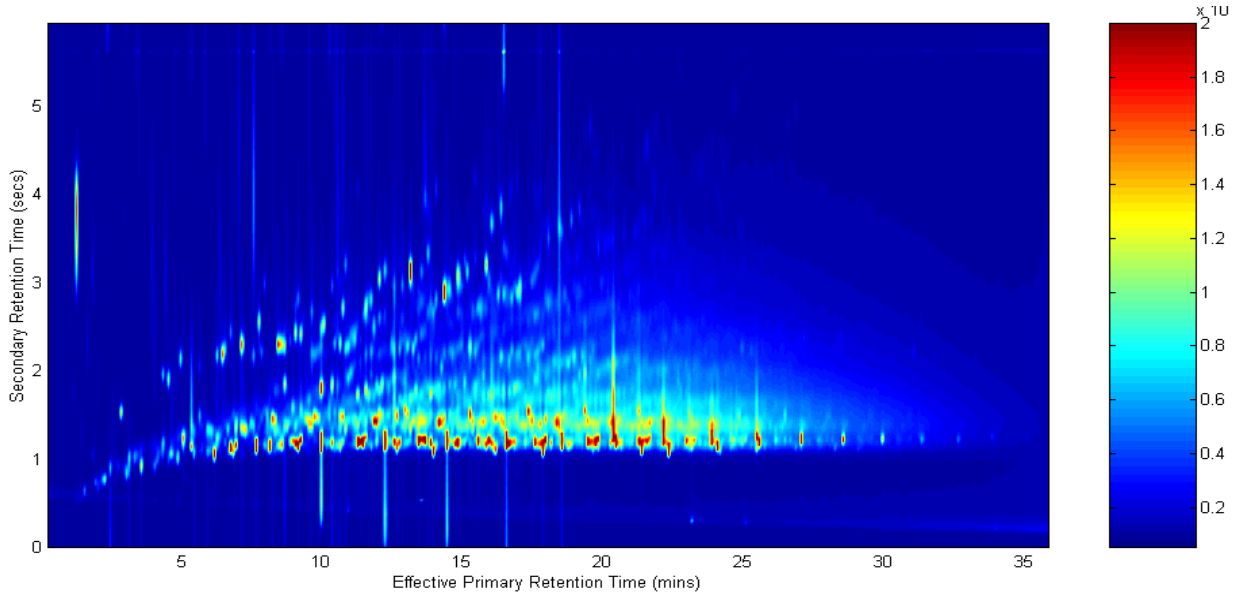

Figure 5-5: A two-dimensional chromatogram of a solution of diesel fuel in CS_2 (1:10 dilution) using CM66.

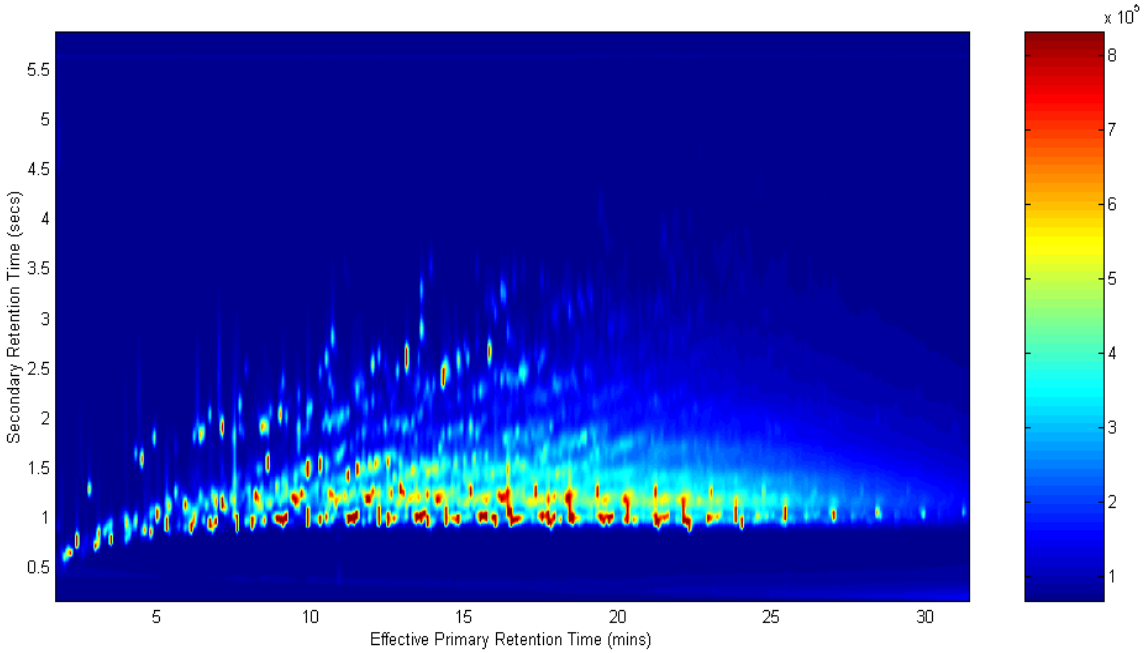

Figure 5-6: A two-dimensional chromatogram of a solution of diesel fuel in CS_2 (1:10 dilution) using CM67

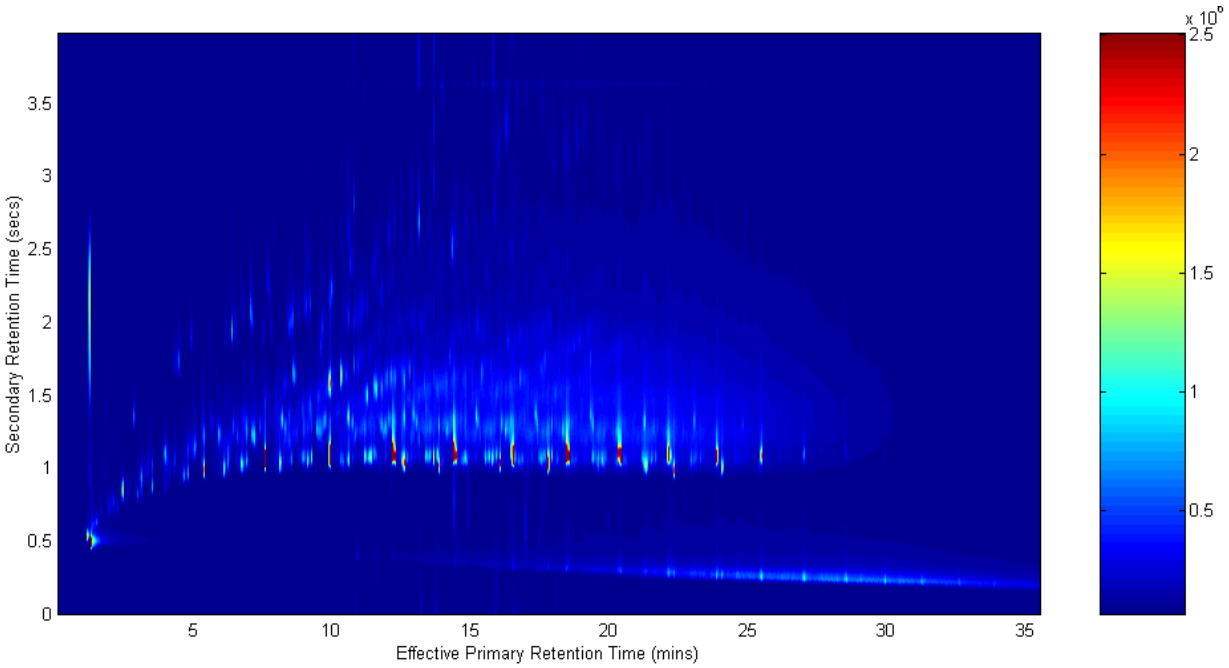

Figure 5-7: A two-dimensional chromatogram of a solution of diesel fuel in CS_2 (1:10 dilution) using CMt66

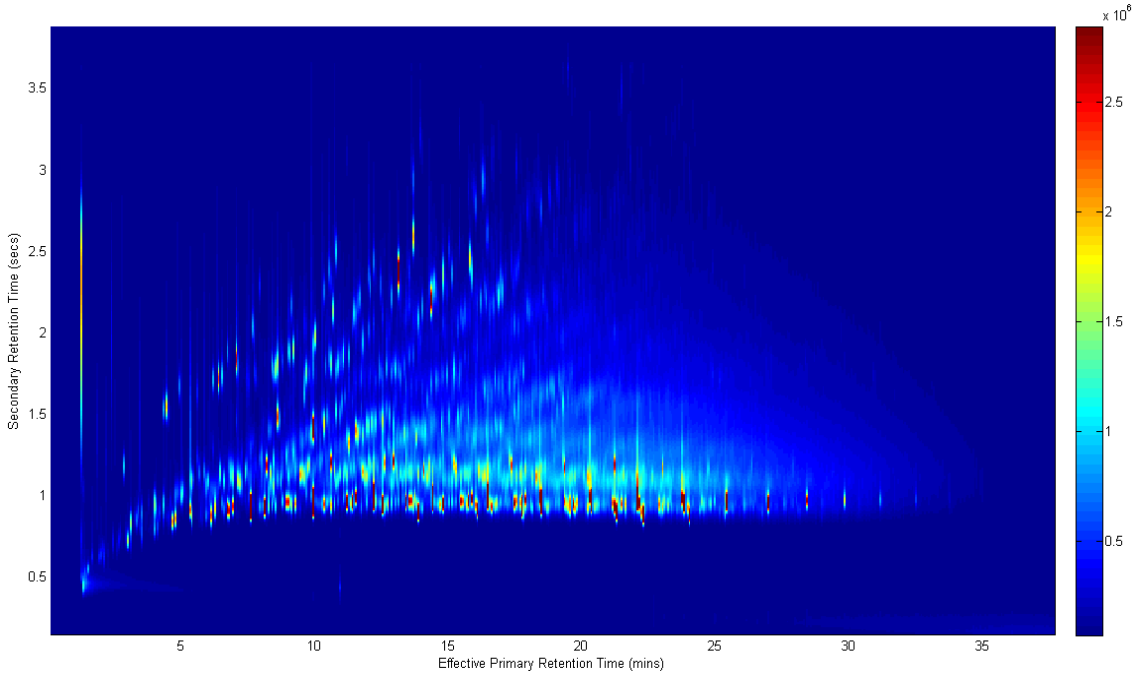

Figure 5-8: A two-dimensional chromatogram of a solution of diesel fuel in CS_2 (1:10 dilution) using CMt67

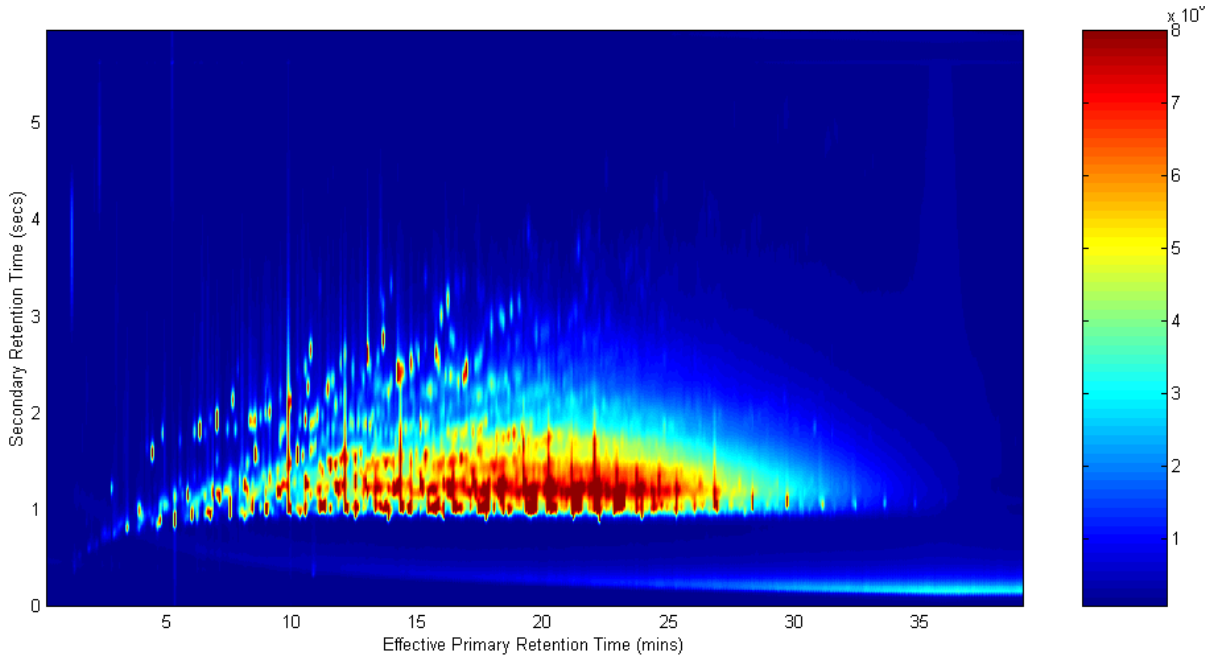

Figure 5-9: A two-dimensional chromatogram of a solution of diesel fuel in CS_2 (1:10 dilution) using CMS66

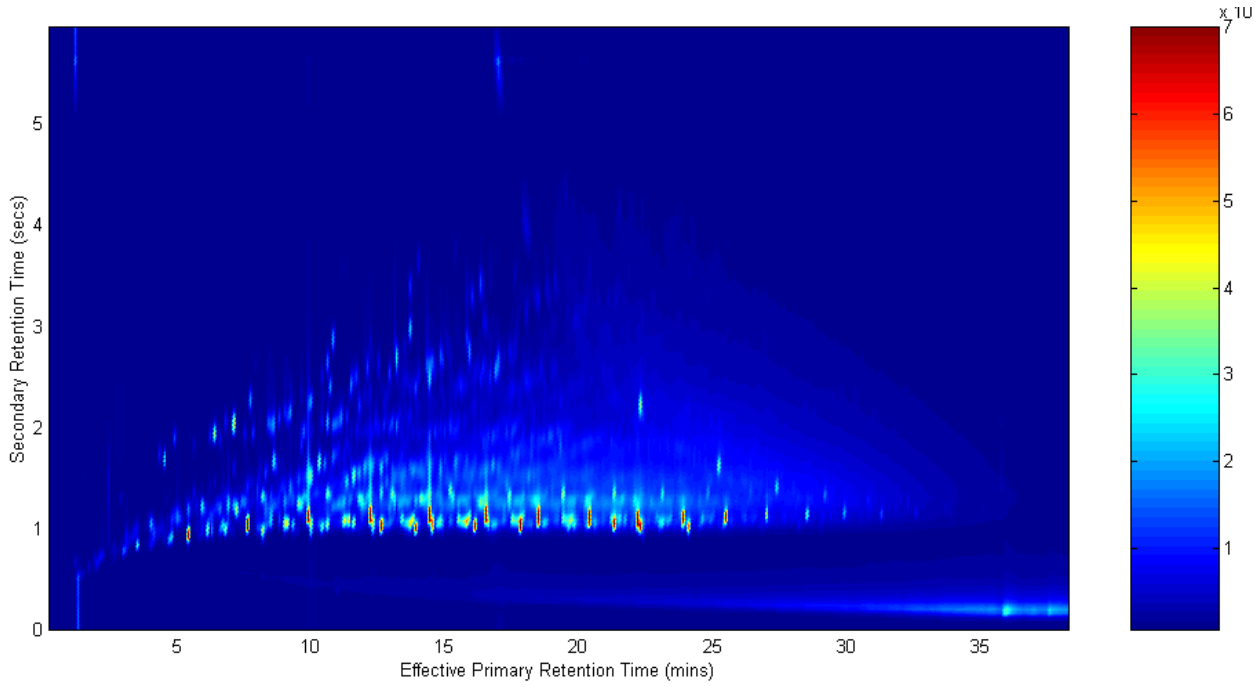

Figure 5-10: A two-dimensional chromatogram of a solution of diesel fuel in CS_2 (1:10 dilution) using CMS67

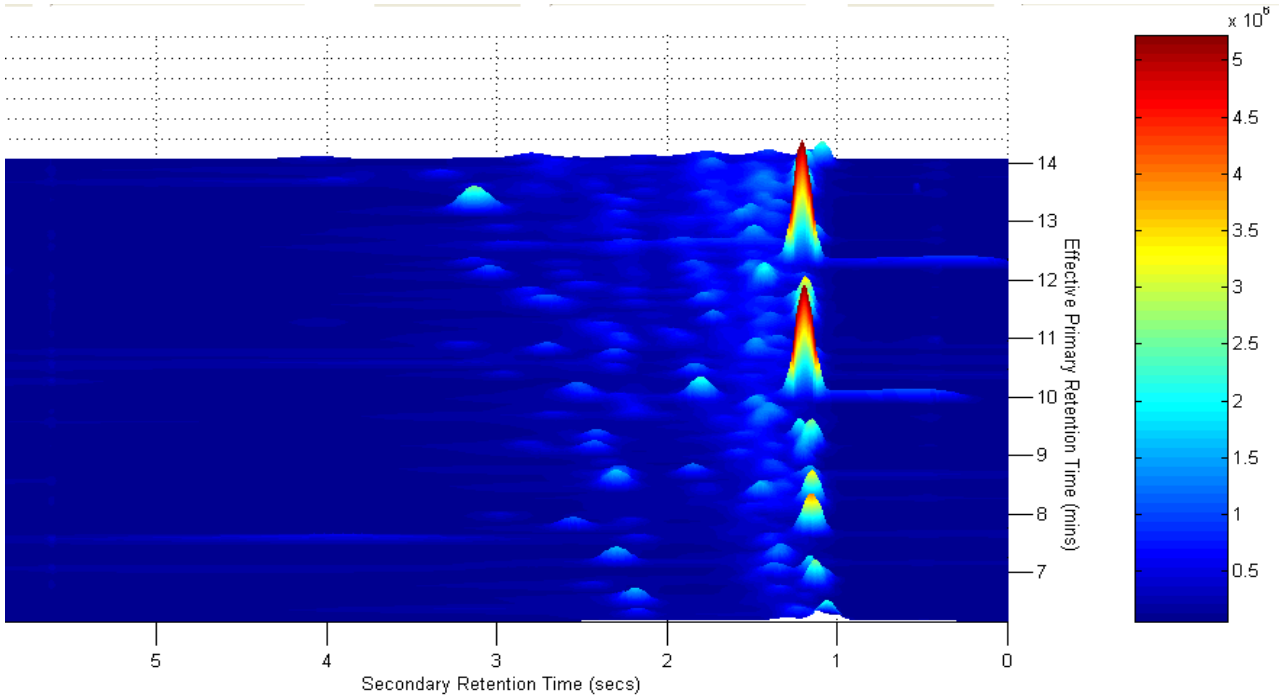

Figure 5-11: Three dimensional view of diesel fuel in CS_2 (10:1 dilution) for the CM66 modulator

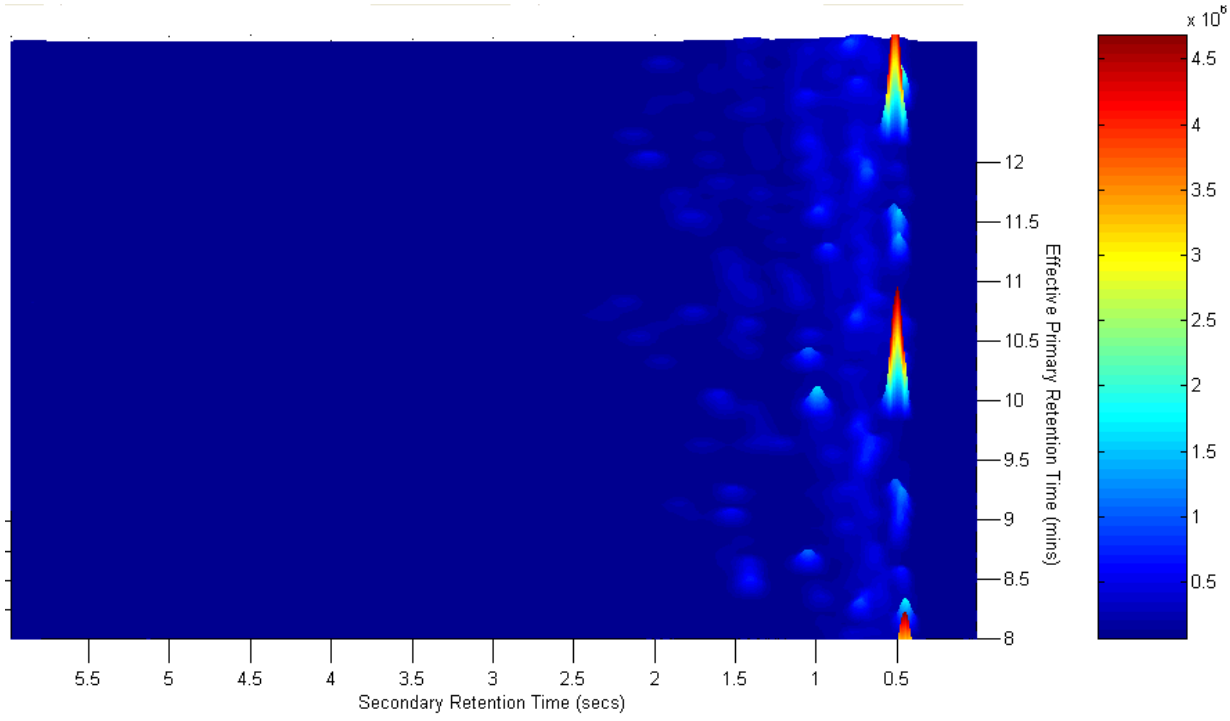

Figure 5-12: Three dimensional view of diesel fuel in CS_2 (10:1 dilution) for the CM67 modulator

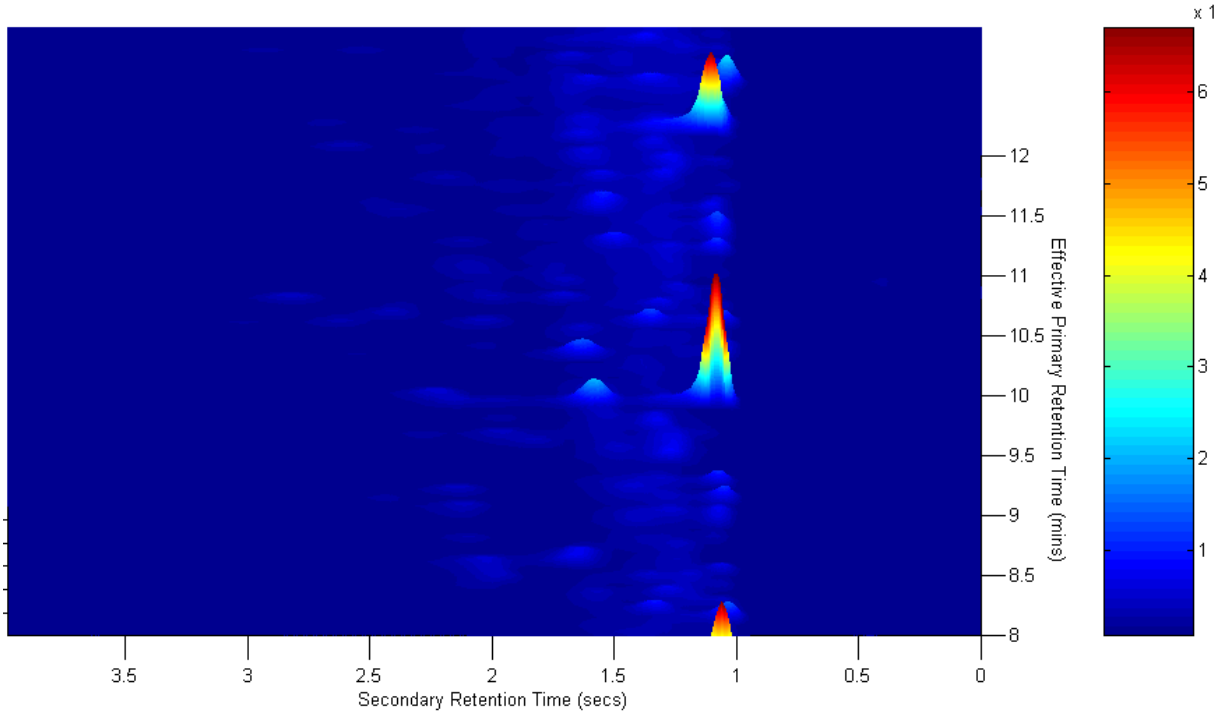

Figure 5-13: Three dimensional view of diesel fuel in CS_2 (10:1 dilution) for the CMt66 modulator

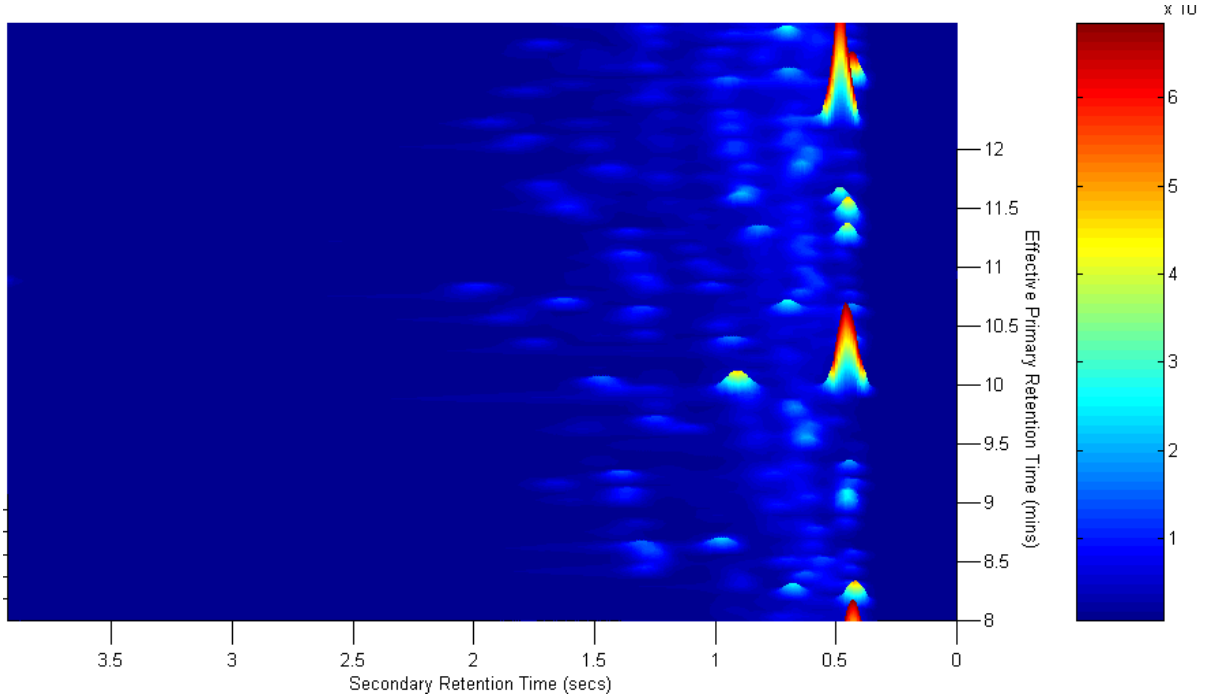

Figure 5-14: Three dimensional view of diesel fuel in CS_2 (10:1 dilution) for the CMt67 modulator

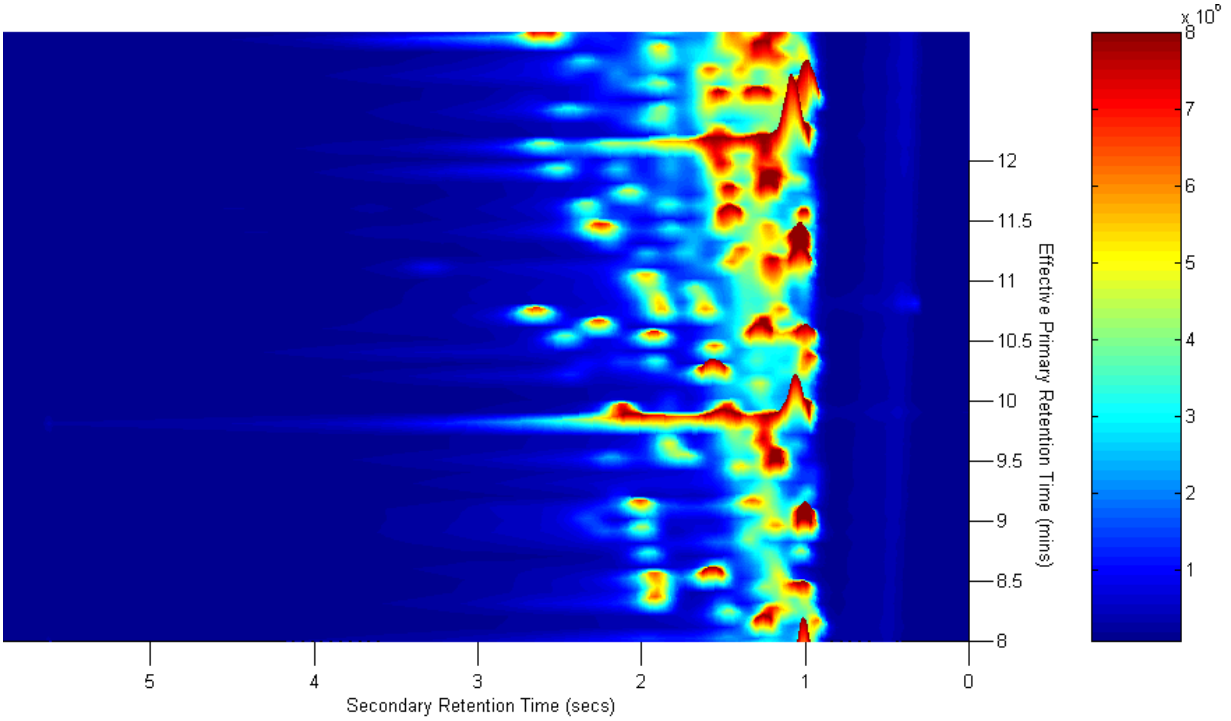

Figure 5-15: Three dimensional view of diesel fuel in CS_2 (10:1 dilution) for the CMS66 modulator

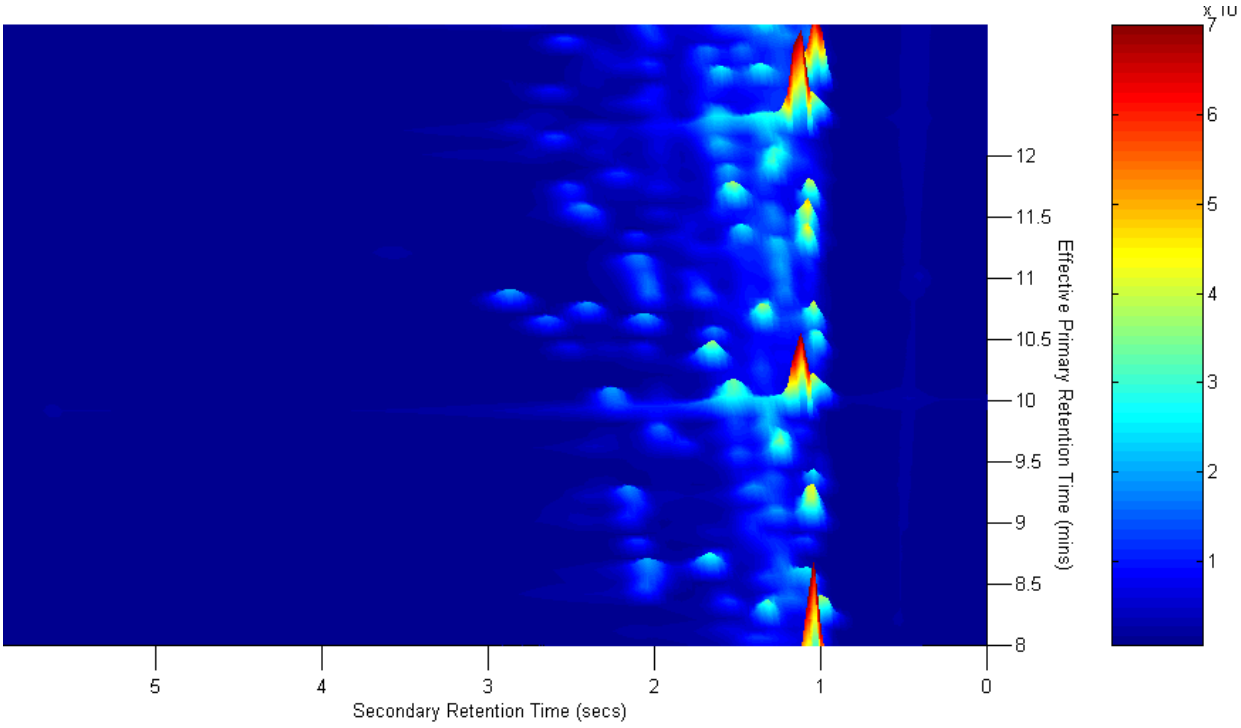

Figure 5-16: Three dimensional view of diesel fuel in CS_2 (10:1 dilution) for the CMS67 modulator

Overall, the most significant improvement to the peak widths at half height was with the largest restriction. Increasing the total length of the modulator provided some improvement to the peak widths at half height. The thin walled modulator provided an improvement in the peak widths at half height as well, but in addition to that also allowed for a decrease in the modulation period.

Chapter 6
Robustness of a Single Stage Modulator

The modulator has been hailed as the heart of a GC × GC system. As such, any failure in the modulator critically affects the instrument. The robustness of the modulator is thus a key issue of concern.

As previously stated, the robustness of the single stage modulator should ideally improve upon that of the dual stage modulator as a result of the removal of the middle contact from the body of the modulator. By doing so, this helps to limit manufacturing problems as well as create a simplified interface for routine use, making it less susceptible to damage. As the 2D-TAG system requires experiments to be run unimpeded for weeks at a time, the single stage modulator would be an ideal alternative to the dual stage modulator with respect to robustness. However, before the single stage modulator could be deemed superior, its robustness needed to be tested.

Using a standard of n-$C_{16}H_{34}$ and n-$C_{20}H_{42}$ in CS_2, the single stage modulator was run continuously for one week. Furthermore, to ensure that reproducible results were produced and that the experiments were continuously active, an auto sampler was utilized.

Over the course of the week, results from the modulator proved to be very consistent. The tallest peaks from each of the three compounds were used in order to find the peak height. The peak height for the n-C_{16} was approximately 1,100 000 at the beginning of the week and 1,000,000 at the end of the week as seen in Figure 6-1. As for the n-C_{20} (Figure 6-2) peak heights, approximately 280,000 was observed at the beginning of the week, while the height at the end of the week was 260,000. For the n-C_{16} and n-C_{20} peaks, the peak heights and shapes

remained similar throughout the week. Overall the peak shapes were consistent throughout the week as well as the peak heights.

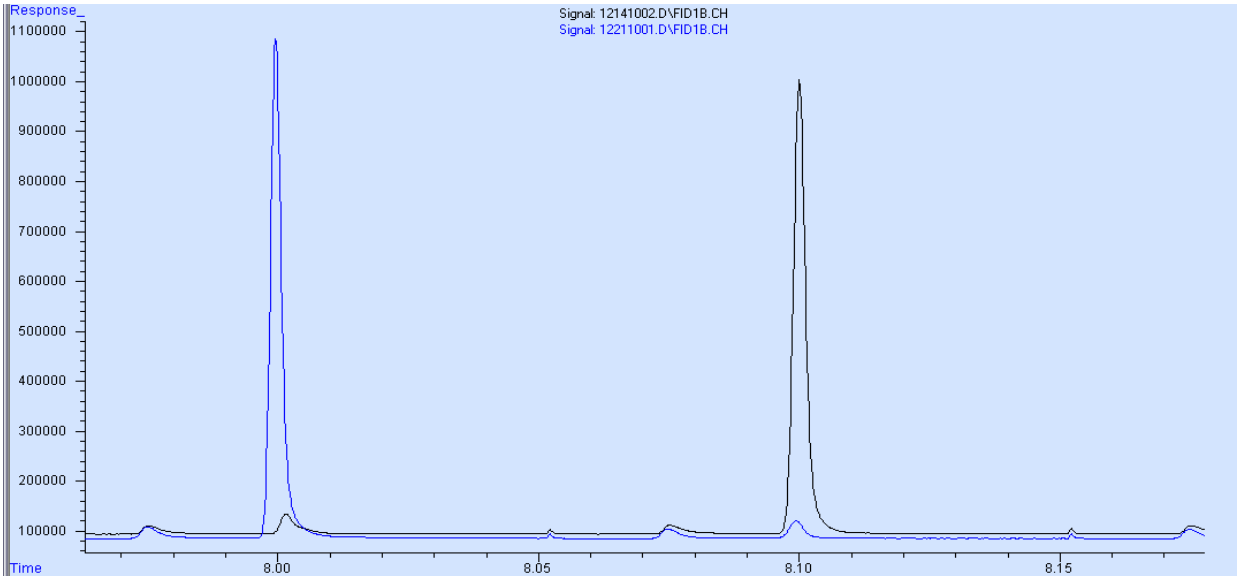

Figure 6-1: Chromatogram of C_{16} at the beginning of the robustness test in black (right) and end of the test in blue (left)

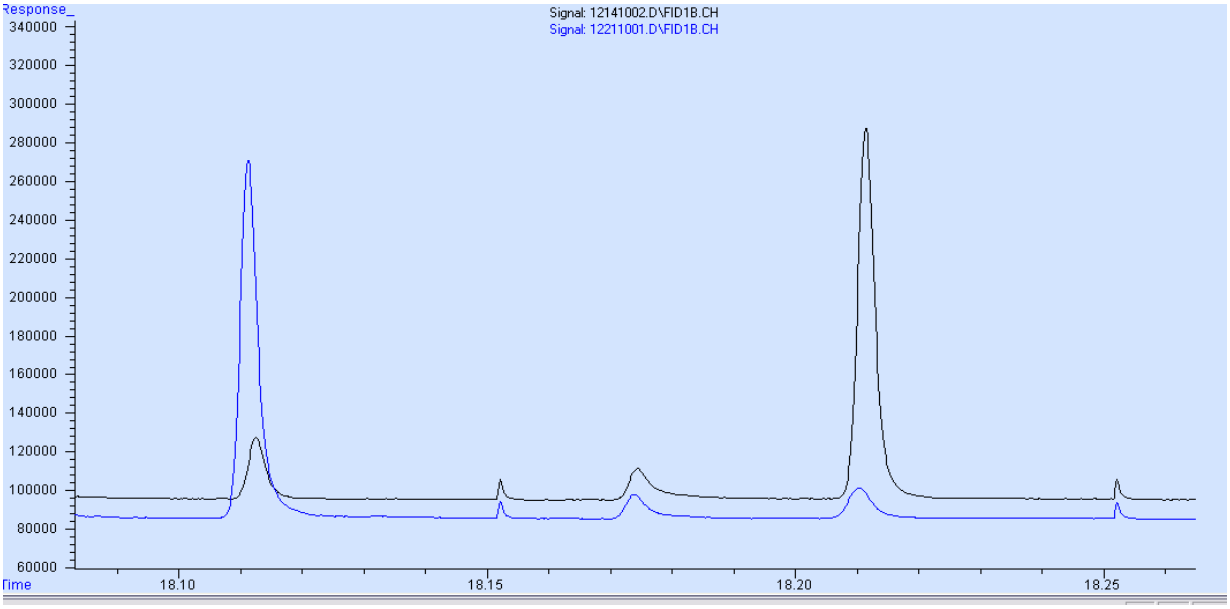

Figure 6-2: Chromatogram of C_{20}, at the beginning of the robustness test in black (right) and end of the test in blue (left**)**

Chapter 7
Conclusions

The main focus of this thesis was to further develop and improve upon the design of the modulator outlined in Ognjen Panic's Masters Thesis. A number of modifications were made, which improved the effectiveness and robustness of the 2D-TAG system. First, the modulator was developed with a decrease in wall thickness. This allowed for the modulator's cool down time to be reduced to less than two seconds, which, in turn, allowed shorter modulation periods (a reduction from a minimum of 6 s for the thick-walled modulator to 2 s for the thin-walled one). The second improvement involved the removal of the middle contact. This resulted in the conception of the single stage modulator model without the breakthrough problem. The design was simpler to manufacture and more robust than the dual stage model as the attachment of the middle contact proved to be problematic. Testing of the single stage modulator was conducted to determine whether it could meet the requirements of the 2D-TAG system. The modulator was able to perform well over a week of continuous use with little to no degradation of the peaks. Field tests performed by the Berkeley group confirmed that the single stage modulator is very robust and can be used without any problems for periods of time significantly longer than a typical field campaign.

A comparison of the signal-to-noise ratio between 2D-GC and conventional 1D-GC was also completed. It was determined that the there was an improvement of at least one order of magnitude in favour of 2D-GC over 1D-GC.

References

1. Takegawa, N., Miyazaki, Y., Kondo, Y., Komazaki, Y., Miyakawa, T., Jimenez, J. L., Jayne, J. T., Worsnop, D. R., Allan, J. D, and Weber, R. J. "Characterization of an Aerodyne Aerosol Mass Spectrometer (AMS): Intercomparison with Other Aerosol Instruments", Aerosol Science and Technology, 39:760–770, 2005

2. Welthagen, W.; Schnelle-Kreis, J.; Zimmermann, R., Search criteria and rules for comprehensive two-dimensional gas chromatography–time-of-flight mass spectrometry analysis of airborne particulate matter, J. Chromatog. 2003, 1019: 233–249

3. Pope, C. A., Dockery, D. W., Health Effects of Fine Particulate Air Pollution: Lines that Connect, J. Air and Waste Manage. Assoc. 2006, 56: 709-742.

4. Cass, G. R., Organic molecular tracers for particulate air pollution sources, Trends Anal. Chem. 17 (6) 1998 356-366.

5. Goldstein, A. H.; Worton, D.R.; Williams, B. J.; Hering, S. V.; Kreisberg, N. M.; Panić, O.; Górecki, T., Thermal desorption aerosol comprehensive two-dimensional gas chromatographic resolution for in-situ measurements of organic aerosols, J. Chromatog. A, 2008 1186:.340-347

6. Namiesnik, J., Zabiegala, B., Kot-Wasik, A., Partyka, M., Wasik, A., Passive sampling and/or extraction techniques in environmental analysis: a review, Anal Bioanal Chem 2005 381: 279-301.

7. Seethapathy, S., Gorecki, T., Li, X., Passive sampling in environmental analysis, J. Chromatog. A, 2008 1186: 234-253.

8. Williams, B. J.; Goldstein, A. H.; Kreisberg, N. M.; Hering, S. V., An In-Situ Instrument for Speciated Organic Composition of Atmospheric Aerosols: Thermal Desorption Aerosol GC/MS-FID (TAG). Aerosol Sci. Technol. 2006, 40: 627-638.

9. Panić, O. Development of a Cost-Effective and Consumable-Free Interface for Comprehensive Two-Dimensional Gas Chromatography (GC×GC). M.Sc. Thesis, presented at the University of Waterloo, 2007.

10. Górecki, T.; Harynuk, J.; Panić, O. The evolution of comprehensive two-dimensional gas chromatography (GC × GC). J. Sep. Science 5-6/2004, 359-366.

11. Górecki, T.; Panić, O.; Oldridge, N. Recent advances in comprehensive two-dimensional gas chromatography (GC × GC). J. Liq. Chromatogr. A 2006, 29: 1077-1083.

12. Liu, Z.; Phillips, J. B. Comprehensive two-dimensional gas chromatography using an on-column thermal modulator interface. J. Chromatogr. Sci. 1991, 29 (6), 227–231.

13. Phillips, J. B.; Ledford, E. B. Thermal modulation: A chemical instrumentation component of potential value in improving portability. Field Anal. Chem. Tech. 1996, 1 (1), 23–29.

14. Phillips, J. B.; Gaines, R. B.; Blomberg, J.; van der Wielen, F. W. M.; Dimandja, J-M.; Green, V.; Granger, J.; Patterson, D.; Racovalis, L.; de Geus, H. J.; de Boer, J.; Haglund, P.; Lipsky, J.; Sinha, V.; Ledford, E.B., Jr. A robust thermal modulator for comprehensive two-dimensional gas chromatography. J. High. Resol. Chromatogr. 1999, 22 (1), 3–10.

15. Kinghorn, R. M.; Marriott, P. Comprehensive two-dimensional gas chromatography using a Modulating Cryogenic Trap. J. High Resol. Chromatogr. 1998, 21 (11), 620–622.

16. Ledford, E. B., Jr.; Billesbach, C. Jet-cooled thermal modulator for comprehensive multidimensional gas chromatography. J. High Resol. Chromatogr. 2000, 23 (3), 202–

17. Harynuk, J.; Górecki, T. Design considerations for a GC _ GC system. J. Sep.Sci. 2002, 25 (5–6), 304–310.Beens, J.; Adachour, M.; Vreuls, R.J.J.; van Altena, K.;

18. Brinkman, U. A. Th. Simple, non-moving modulation interface for comprehensive two-dimensional gas chromatography. J. Chromatogr. A 2001, 919 (1), 127–132.Ledford,

19. Ledford, E. B., Jr.; Billesbach, C.; Termaat, J. Pittcon 2002, March 17–22, 2002, New Orleans, LA. Contribution #2262P.

20. Harynuk, J.; Górecki, T. New liquid nitrogen cryogenic modulator for comprehensive two-dimensional gas chromatography. J. Chromatogr. A 2003, 1019 (1–2), 53–63.

21. Sacks, R.; Libardoni, M.; Waite, J.H. Electrically heated, air-cooled thermal modulator and at-column heating for comprehensive two-dimensional gas chromatography. Anal. Chem. 2005, 77 (9), 2786–2794.

22. Libardoni, M.; Hasselbrink, E.; Waite, J.; Sacks, R. At-column heating and a resistively heated, liquid-cooled thermal modulator for a low-resource bench-top GC × GC. J. Sep. Sci. 2006, 29, 1001-1008

23. Kim, S., Reidy, S. M., Block, B. P., Wise, K. D., Zellers, E. T., Kurabayashi, K. Microfabricated thermal modulator for comprehensive two-dimensional micro gas chromatography: design, thermal modeling, and preliminary testing. Lab Chip 2010, 10, 1647-54.

24. Bruckner, C. A.; Prazen, B. J.; Synovec, R. E. Comprehensive two-dimensional high-speed gas chromatography with chemometric analysis. Anal. Chem. 1998, 70, 2796–2804.

25. Seeley, J. V.; Kramp, F.; Hicks, C. J. Comprehensive two-dimensional gaschromatography via differential flow modulation. Anal. Chem. 2000, 72, 4346–4352.

26. Bueno, P. A.; Seeley, J. V., Jr. Flow-switching device for comprehensive two dimensional gas chromatography. J. Chromatogr. A 2004, 1027 (1–2), 3–10.

27. Micyus, N .J.; McCurry, J. D.; Seeley, J. V. Analysis of aromatic compounds in gasoline with flow-switching comprehensive two-dimensional gas chromatography. J. Chromatogr. A 2005, 1086 (1–2), 115–121.

28. www.exair.com (Nov 13, 2007)

29. Grob, R. L., Barry, E. F., Modern Practice of Gas Chromatography. John Wiley and Sons, Inc, Hoboken, New Jersey. 2004, 57-69, 136-137

30. Williams B. J., Goldstein A. H., Kreisberg N. M., Hering S. V. TI: Hourly Speciated Organic Aerosol Composition in Riverside, CA during SOAR 2005. Aerosol Sci & Tech, 2006, 40:627-638.

31. Lee A. L., Lewis A. C., Bartle K. D. E., McQuaid J. B., Marriott P. J. A comparison of modulating interface technologies in comprehensive two-dimensional gas chromatography (GC×GC). J Microcol Sep 2000, 12(4):187-193.

32. Marriott P. J., Ong R. C. Y., Kinghorn R. M., Morison P.D. Time-resolved cryogenic modulation for targeted multidimensional capillary gas chromatography analysis. J Chromatogr A 2000, 892(1-2):15-28.

33. U.S. Environmental Protection Agency, Part 136, Appendix B, Revision 1.11, 40 CFR.; Ch 1, 1986, p. 537-539, at URL http://ecfr.gpoaccess.gov/cgi/t/text/text-idx?c=ecfr&sid=44c46aef5b71fe4102de80b1b36cad17&rgn=div5&view=text&node=40:22.0.1.1.1&idno=40#40:22.0.1.1.1.0.1.7.2, accessed on December 10, 2010.